JOC Perspective

pubs.acs.org/joc

Capturing the Essence of Organic Synthesis: From Bioactive Natural Products to Designed Molecules in Today's Medicine†

Arun K. Ghosh*

Departments of Chemistry and Medicinal Chemistry, Purdue University, 560 Oval Drive, West Lafayette, Indiana 47907

akghosh@purdue.edu

Received August 16, 2010

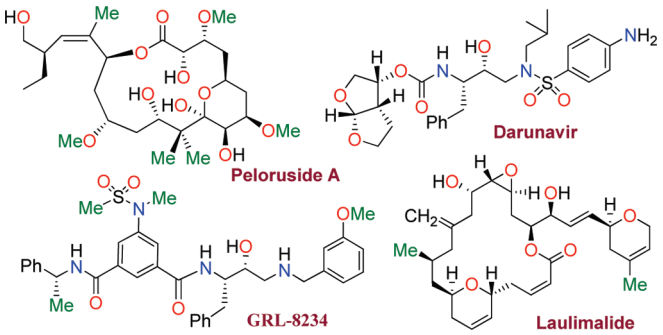

In this Perspective, I outline my group's research involving the chemical syntheses of medicinally important natural products, exploration of their bioactivity, and the development of new asymmetric carbon−carbon bond-forming reactions. This paper also highlights our approach to molecular design and synthesis of conceptually novel inhibitors against target proteins involved in the pathogenesis of human diseases, including AIDS and Alzheimer's disease.

Introduction

My long-standing interest has been to harness the power of organic synthesis and address the problems of today's medicine. I have envisioned a broad research program that involves diverse applications of organic synthesis with an emphasis on the exploration of chemistry and biology of natural products as well as the development of conceptually novel molecular probes against target peptides and proteins implicated in the pathogenesis of human diseases. Our goal was a strong and vigorous synthetic program that would complement and fuel our hypotheses and molecular design capabilities. I have assembled a multidisciplinary collaboration involving organic chemistry, biology, and medicine. This exciting interdisciplinary research endeavor has presented excellent learning opportunities and provided solid ground for teaching and training students in the laboratory.

Synthetic organic chemistry is, indeed, an enabling science, particularly when dealing with critical issues of biology and medicine. The advent of sophisticated technologies and advances in molecular biology have brought unique perspectives to modern research in human health and medicine. For example, the molecular insights derived from our X-ray crystal structures of protein−ligand complexes have greatly advanced our design capabilities. This, in turn, led to important new challenges and further opportunities for organic synthesis. The understanding of human diseases at the molecular level, their pathogenesis, and identification of biological target led to the possibility that one could design and develop selective molecular therapeutics for novel treatments. Selectivity may well prove to be one of the most important factors in minimizing toxicity and side effects of treatments.

Bioactive natural products have had a dramatic impact in medicine and society.[2] They display a seemingly endless structural diversity and are often found only in miniscule quantities. Inspiration from natural products has also brought new perspectives to organic synthesis. The last 50 years or so have witnessed revolutionary progress in natural product isolation, structural elucidation, total syntheses, and biological studies. Many times, I have been asked how I choose my molecular targets. It seems often that it is the unique structural features of molecules such as hapalosin or madumycin that is of first attraction. Sometimes it is the unusual biological properties or mode of action as with laulimalide or pelorusides. Other times, it is the unknown that draws us in, as with those compounds nature manufactures in only the tiniest amounts. The study of

† Dedicated to my colleague, Professor Ei-ichi Negishi, with deep respect and admiration.

DOI: 10.1021/jo101606g Published on Web 10/11/2010

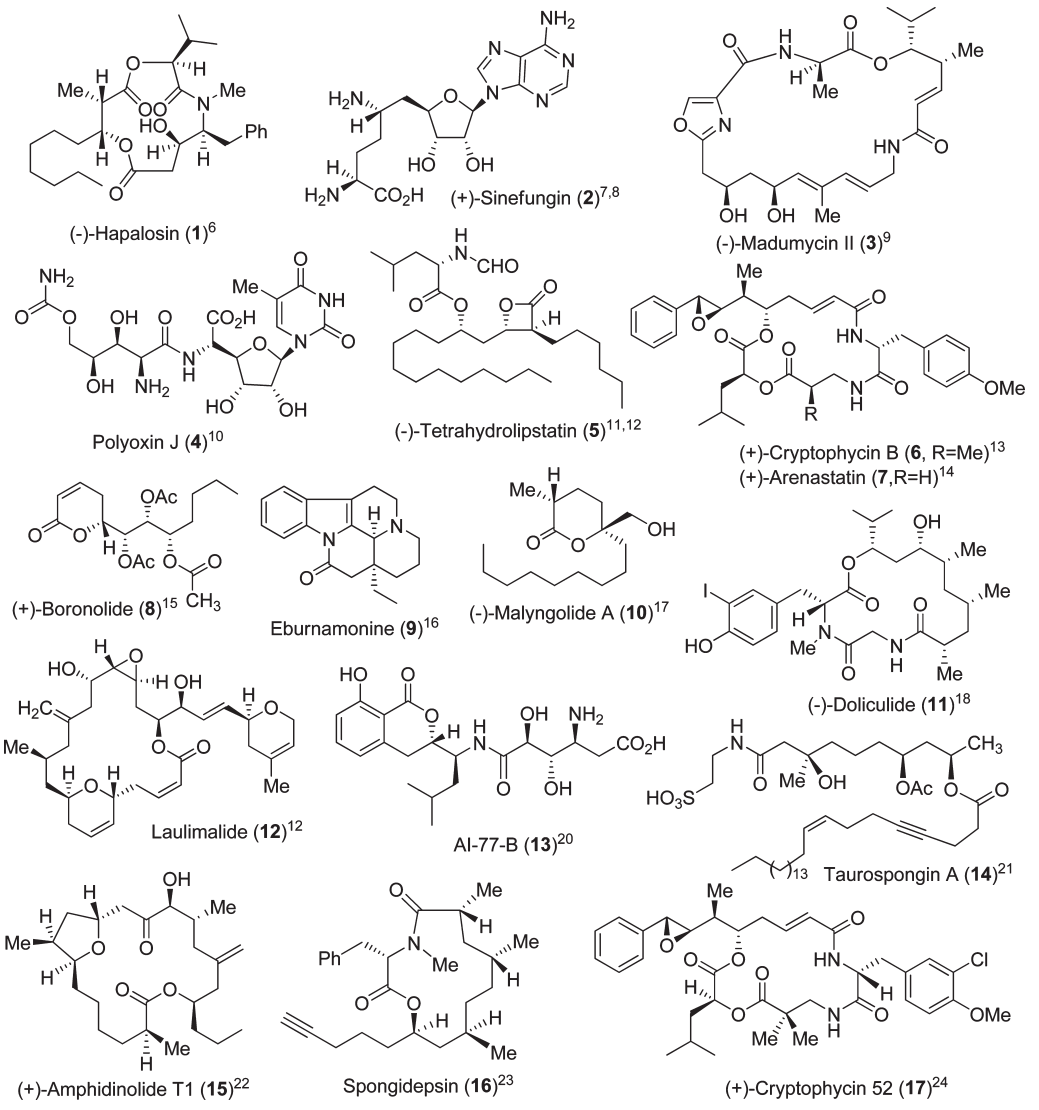

FIGURE 1. Bioactive natural product targets synthesized by the Ghosh group, from 1996 to 2003.

these rare natural products has motivated our development of new and efficient chemistry for synthesis. Organic synthesis is also at the epicenter of our medicinal research. The design of new molecular probes as well as improvements of selectivity and potency require the synthesis of stereochemically defined novel structural motifs, scaffolds, and functionalities. In this paper, we provide a brief overview of our research program which encompasses total syntheses and biological studies of a range of bioactive natural products, the development of new synthetic methodologies, and our perspectives in the design and synthesis of conceptually novel enzyme inhibitors for possible treatment of AIDS and Alzheimer's disease. In light of our recent review,[1] the latter part will be reviewed only briefly. Also, it is beyond the scope of this paper to include a comprehensive citation of all related natural product syntheses. Only selected references have been included in the context of highlighting areas of particular biological or synthetic relevance.

Highlights in Natural Product Synthesis and Exploration of Biology

Natural products display an incredible range of structural diversity and often possess intriguing biological properties.[2,3] In fact, many of today's approved drugs are either natural product-derived or have been developed on the basis of natural product lead structures.[4,5] One of our main research objectives is to carry out the synthesis of rare and scarce natural products of biological relevance and then investigate their mode of action to obtain insight. Since our first synthesis of hapalosin (**1**) in 1996, my laboratory has carried out the synthesis of a range of medicinally important and structurally diverse natural products shown in Figures 1 and 2.[6−35]

Hapalosin (**1**) is a cyclodepsipeptide that displays intriguing multidrug-resistance reversing activity by inhibiting P-glycoprotein.[36] Our synthesis featured Evans's asymmetric *syn*-aldol reaction[37] utilizing (1*S*,2*R*)-aminoindanol-derived oxazolidinone as the chiral auxiliary.[6] As shown in Figure 3, the aldol reaction with chiral imide **30** and *n*-octanaldehyde provided aldol product **31** in 90% yield as a single diastereomer. A highly diastereoselective synthesis of the statine derivative was carried out by $NaBH_4$ reduction of amino ketone **33** in propanol at 0 °C to provide the corresponding amino alcohol as a mixture (5:1) of diastereomers in 73% yield. This was converted to protected statine

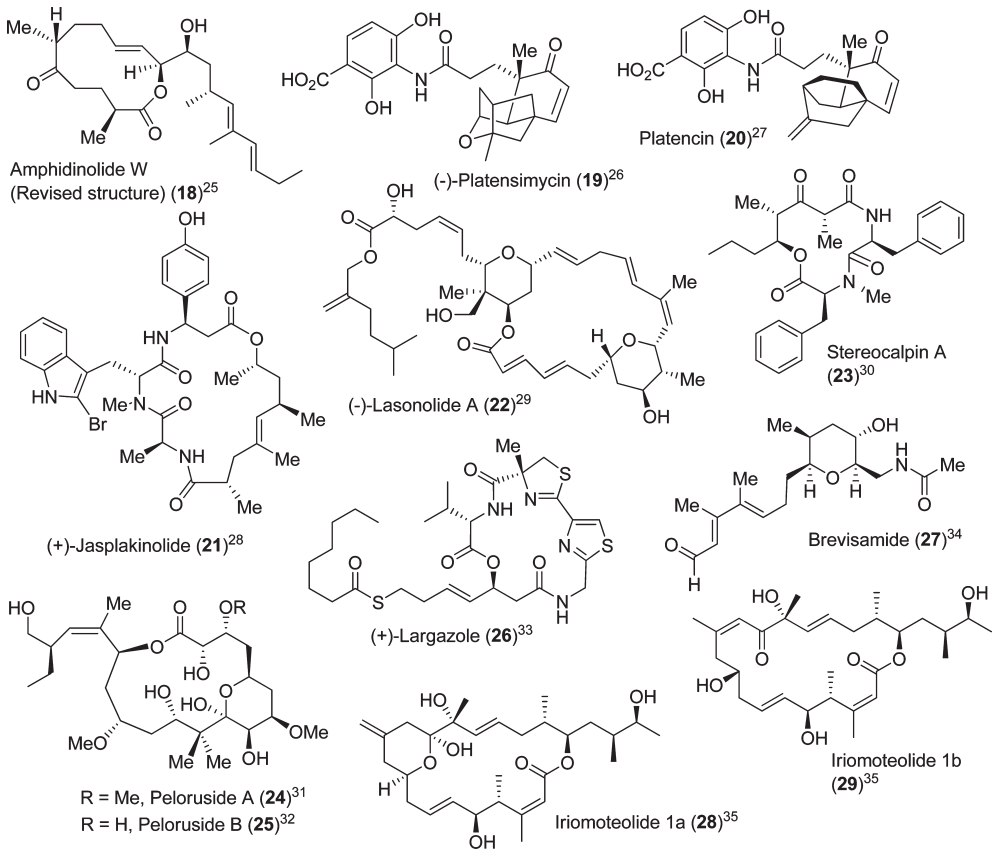

FIGURE 2. Bioactive targets synthesized by the Ghosh group, from 2005 to date.

derivative **34**. Assembly of fragments, cycloamidation, and removal of the protecting groups provided (−)-hapalosin. Other syntheses[38] and detailed structure−activity studies of hapalosin were subsequently carried out.[39]

Sinefungin (**2**) is an interesting nucleoside with structural similarities to *S*-adenosylmethionine (SAM).[40] Sinefungin exhibits a range of biological activity including antifungal, antiviral, and antiparasitic properties. The biological mechanism of action is related to the inhibition of SAM-dependent methyltransferase enzymes. Despite the intriguing bioactivity, sinefungin could not be used clinically because of its *in vivo* toxicity, possibly due to its lack of selectivity against MTases.[41] Structural modifications may lead to an improvement in selectivity. This has been an active area of investigation by many research groups.[42]

Our synthesis of sinefungin (Figure 4) features a highly diastereoselective alkylation of D-ribose and (1*S*,2*R*)-aminoindanol-derived chiral oxazolidinone **36** to provide **37** in 78% yield as a single diastereomer.[7] A Curtius rearrangement installed the C-6 amino stereochemistry. The C-9 amino acid stereochemistry was established by a chiral bisphosphinorhodium complex-catalyzed asymmetric hydrogenation[43] of α-acylaminoacrylate derivative **38**, providing **39** in 95% yield as a single isomer (98% de) by chiral HPLC analysis. Adenylation of acetate derivative **40** using Vorbruggen's conditions,[44] TMSOTf with N^6-benzoyladenine derivative **41** provided β-nucleoside **42** in 93% yield. This was then converted to sinefungin after removal of the protecting groups. Additionally, the synthesis provided access to a variety of structural variants of sinefungin. We have also carried out a formal synthesis of sinefungin utilizing an efficient elongation of protected ribose derivative **43**.[8] As shown in Figure 5, reaction of triflate **43** with an alkynyllithium reagent in the presence of 1,3-dimethylpropyleneurea (DMPU) provided alkyne derivative **44** in 86% yield. Removal of the TBS group and LAH reduction afforded *E*-allylic alcohol **45** exclusively. Sharpless asymmetric epoxidation[45] followed by regioselective epoxide opening[46] provided azidodiol **46**, which was converted to sinefungin.

Sinefungin is an inhibitor of MTase, and recently, a sinefungin-bound X-ray crystal structure of MTase has been determined by collaborators Dong and Li at the Wadsworth Center in New York.[47] The structure provided important molecular insights for designing less toxic and more selective sinefungin-based novel inhibitors. Both syntheses of sinefungin are being utilized for the design and synthesis of the next generation of inhibitors in our laboratories.

We became interested in madumycin II (**3**) synthesis because of its effectiveness against *methicillin-resistant S. aureus* or MRSA, a drug-resistant bacteria that is resistant to all current antibiotics except vancomycin. However, vancomycin is burdened with many serious side effects.[48] A number of derivatives of madumycin II underwent clinical evaluation.[49] We carried out an enantioselective synthesis for the possible preparation of structural analogues which could not be derived from natural products.[9] As shown in Figure 6, the synthesis is highlighted by the development of a 1,3-*syn*-diol segment in enantiomerically pure form utilizing an enzymatic desymmetrization of a cyclopentane *meso*-diacetate as the key step. Optically active derivative **47** could be prepared

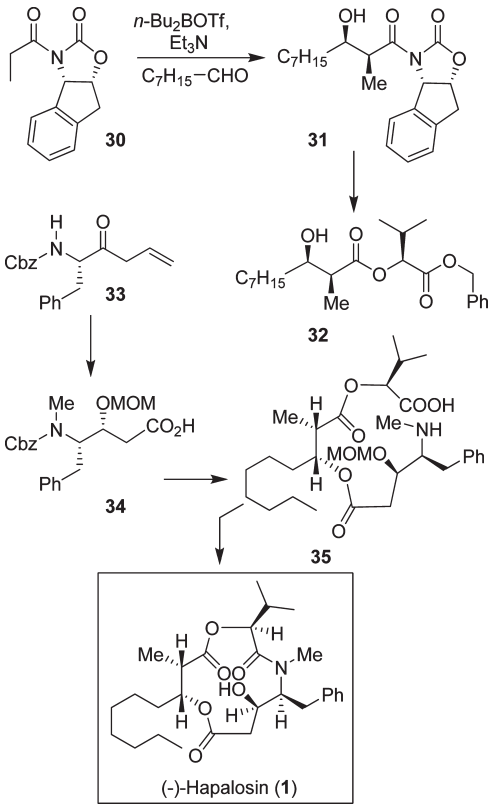

FIGURE 3. Synthesis of (−)-hapalosin (**1**).

in multigram quantities. Ozonolysis followed by $NaBH_4$ reduction and protection of alcohols provided **48**, which was conveniently elaborated to **49**. Oxazole formation was accomplished using Burgess reagent followed by an oxidation to provide **50**. Brown's asymmetric crotylboration was employed to install the C_2- and C_3-stereocenters of madumycin II.

As shown, *syn*-homoallyl alcohol **51** was obtained in 75% yield and high optical purity (>95% ee). It was converted to acid **52**. Coupling of **50** and **52** followed by Yamaguchi macrolactonization of the resulting seco acid provided macrolactone **53**. Deprotection of both MOM-protecting groups was carried out using $n Bu_4N^+Br^-$ and dichlorodimethylsilane to provide madumycin II (Figure 7).

Our synthesis of polyoxin J (**4**) involved a stereoselective *m*-CPBA-promoted electrophilic epoxidation of ribose-derived allylic alcohol **54** (Figure 8), followed by the regioselective epoxide opening with diisopropoxytitanium diazide using Sharpless' conditions.[46] Azido diol **56** was converted to polyoxin C. The synthesis of 5-*O*-carbamoyl polyoxamic acid **57** was stereoselectively prepared using Sharpless' epoxidation[45] of an L-tartrate-derived allylic alcohol and a regioselective epoxide-opening[46] as the key steps. Coupling of polyoxin C and polyoxamic acid (**57**) provided polyoxin J (**4**).

Tetrahydrolipstatin (**5**) is a saturated derivative of lipstatin, which was isolated from *Streptomyces toxytricini* in 1987. It is an inhibitor of pancreatic and gastric lipases that are responsible for the digestion of fat from food. In 2003, it was approved by the FDA under the trade name Orlistat for the treatment of morbid obesity.[50] Furthermore, tetrahydrolipstatin is an inhibitor of fatty acid synthase (FAS), an enzyme responsible for the synthesis of fatty acids in many human carcinomas. FAS is required for tumor cell survival,

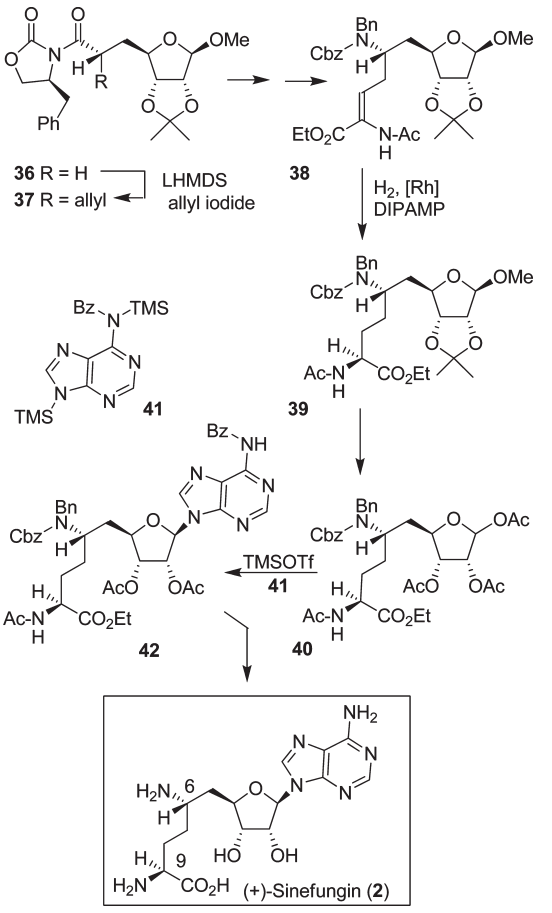

FIGURE 4. Synthesis of (+)-sinefungin (**2**).

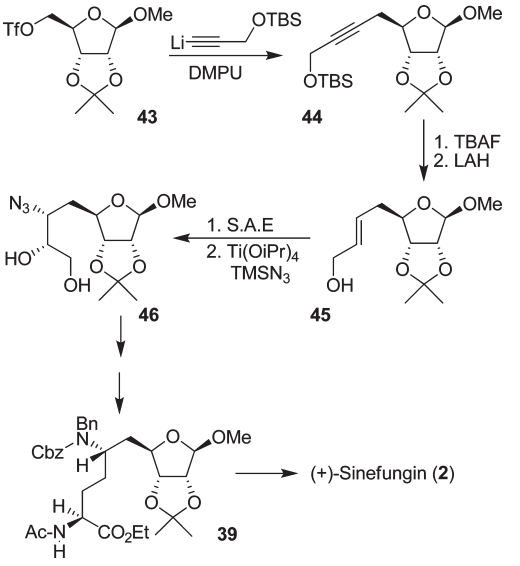

FIGURE 5. Alternative synthesis of sinefungin (**2**).

and therefore, FAS inhibitors have been suggested for cancer chemotherapy.[51] Thus, synthesis of tetrahydrolipstatin and its analogues has become an important area of research. Our first synthesis of tetrahydrolipstatin (**5**) was accomplished using our ester-derived titanium enolate-based diastereoselective *anti*-aldol reaction as the key step.[11]

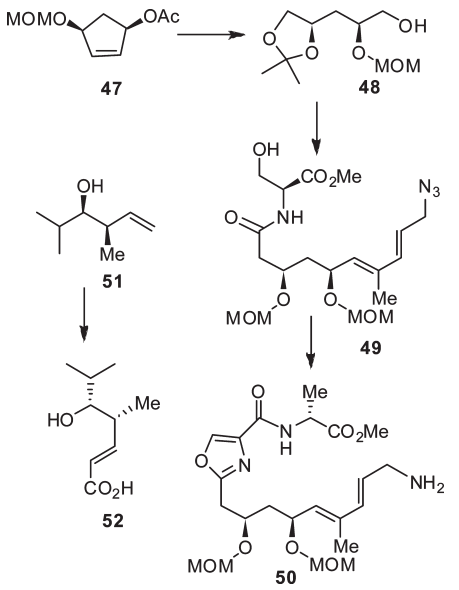

FIGURE 6. Synthesis of the *syn*-1,3-diol unit of madumycin II (**3**).

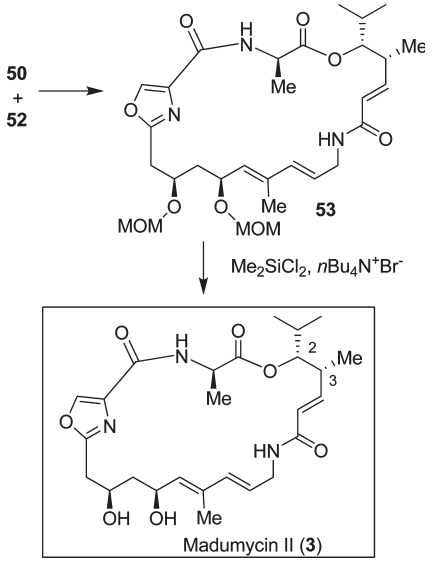

FIGURE 7. Synthesis of madumycin II (**3**).

As shown in Figure 9, an ester−enolate aldol reaction of **58** with cinnamaldehyde provided aldol product **59** as the major diastereomer (6:1 mixture) in 60% yield which was subsequently converted to aldehyde **60**.[11] A nitro aldol reaction was employed to append the requisite carbon chain. Nitro alcohol **61** was converted to *β*-hydroxy ketone **62**, which was subjected to an *anti*-selective reduction using Evans' protocol[52] to provide *anti*-1,3-diol (diastereoselectivity 22:1). It was then converted to tetrahydrolipstatin **5**.

Our recent nonaldol route to *anti*-aldol segments provided more straightforward access to tetrahydrolipstatin and its derivatives.[12b] As shown in Figure 10, alkylated optically active lactone **63** was converted to ketone **65** by DIBAL-H reduction, Horner−Emmons reaction with **64**, followed by oxo-Michael reaction to provide **65**. A chelation-controlled reduction of **65** afforded *syn*-alcohol **66** diastereoselectively (17:1, 88% yield). An acyloxycarbenium ion-mediated

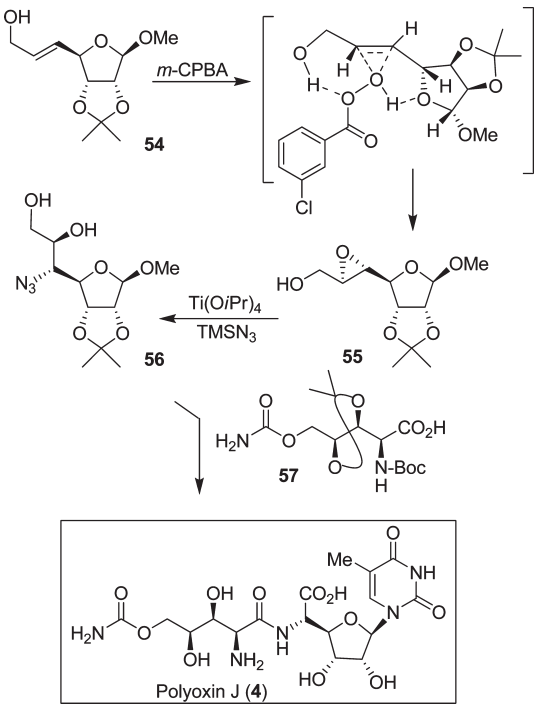

FIGURE 8. Synthesis of polyoxin J (**4**).

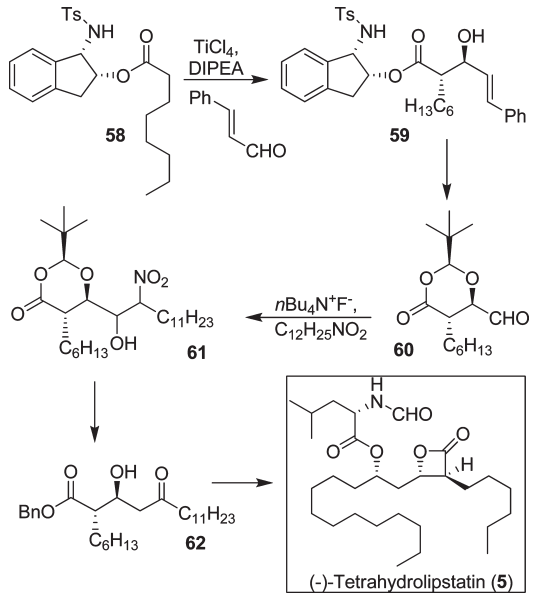

FIGURE 9. Synthesis of (−)-tetrahydrolipstatin (**5**).

ring-opening reaction with 5 mol % of $Zn(OTf)_2$ and Ac_2O provided styrene derivative **67**, which was converted to tetrahydrolipstatin **5**.

Cryptophycins are a group of compounds that exhibit potent antitumor properties. Cryptophycin B (**6**) and arenastatin A (**7**) exhibited IC_{50} values of 7 and 5 pg/mL, respectively, against KB cell lines.[53] Unfortunately, the clinical potential of cryptophycins has been limited due to their degradation in blood caused by the high susceptibility of the ester functionalities to hydrolysis. Therefore, the synthesis of cryptophycin analogues with better *in vivo* stability warranted significant efforts. Cryptophycins exhibit

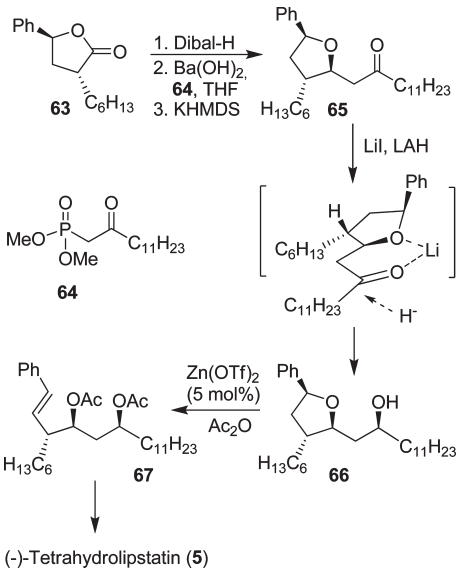

FIGURE 10. Nonaldol route to (−)-tetrahydrolipstatin (**5**).

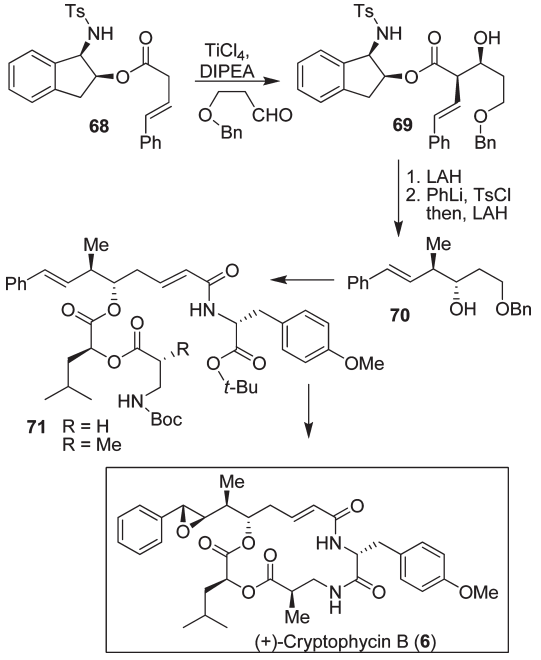

FIGURE 11. Synthesis of (+)-cryptophycin B (**6**).

antiproliferative and antimitotic activity through their interaction with microtubules.[54] One of the synthetic analogues of the cryptophycin class is cryptophycin 52 (**17**), also known as LY355703, which was hydrolytically stable, very potent against numerous tumor cell lines, and underwent clinical development.

Our synthesis of cryptophycin B utilized a highly diastereoselective ester-derived titanium enolate-based *syn*-aldol reaction as the key step.[13] As shown in Figure 11, aldol reaction of ester **68** with 3-(benzyloxy)propanal afforded *syn*-aldol product **69** as a single diastereomer in 98% yield. LAH reduction of **69** gave the corresponding alcohol, which was converted to methyl derivative **70** in a one-pot, two-step sequence involving tosylation with PhLi and *p*-TsCl followed by LAH reduction to provide **70** in 88% overall yield. This

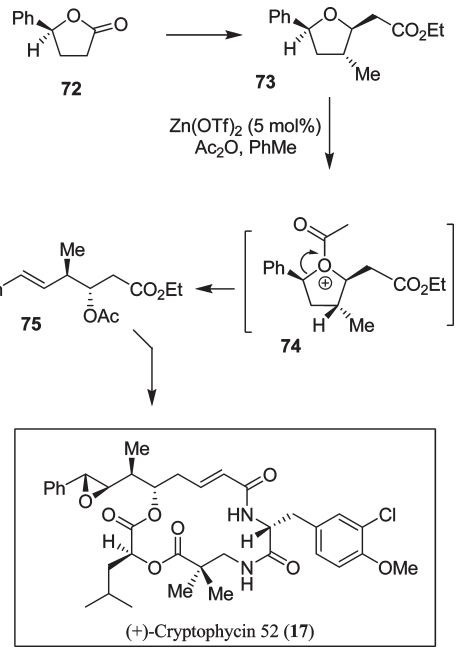

FIGURE 12. Synthesis of (+)-cryptophycin 52 (**17**).

was converted to **71** and then to cryptophycin B (**6**) and arenastatin A (**7**).[14]

We have also accomplished the synthesis of cryptophycin 52 (**17**, LY355703) utilizing an asymmetric nonaldol process for *anti*-aldol variants developed in our laboratory.[24] As shown in Figure 12, both stereogenic centers of the key epoxyoctenamide fragment in **17** were introduced by a diastereoselective alkylation of optically active 5-phenyl-γ-butyrolactone **72**, prepared utilizing CBS-reduction as the key step.[55] Reduction of **72**, Horner−Emmons reaction, followed by oxo-Michael reaction provided **73** diastereoselectively. An acyloxonium ion (**74**) mediated ring-opening of **73** provided **75**, which was converted to cryptophycin 52 (**17**).

Our subsequent synthetic targets were emetic agent boronolide (**8**),[15] antihypertensive agent eburnamonine (**9**),[16] and antibacterial agent (−)-malyngolide (**10**).[17] These were synthesized to feature various synthetic methodologies developed in our laboratories.

We became interested in the synthesis of doliculide (**11**) for a number of reasons. Doliculide exhibits exceedingly potent cytotoxicity against HeLa-S_3 cells with an IC_{50} value of 1 ng/mL.[56] Yamada and co-workers first reported the isolation, initial cytotoxic properties, and synthesis of doliculide.[57] However, its biological mechanism of action was not known. We carried out a new convergent synthesis of doliculide and investigated its biological mode of action in collaboration with Ernest Hamel at the National Cancer Institute.

As shown in Figure 13, the synthesis of the 1,3,5-*syn*/*syn* trimethyl unit started with 4-benzyloxy-3(*S*)-methylbutyronitrile, which was converted to allylic alcohol **76**.[18] Asymmetric cyclopropanation of **76** using a chiral catalyst provided **77** in excellent yield and high diastereoselectivity (91% de).[58] Alcohol **77** was converted to iodide, which upon treatment with *n*-BuLi/TMEDA afforded alkene **78**. Iteration of the same protocol furnished allylic alcohol **79** (Figure 14). The 1,3-*syn*-diol functionality was introduced by Sharpless

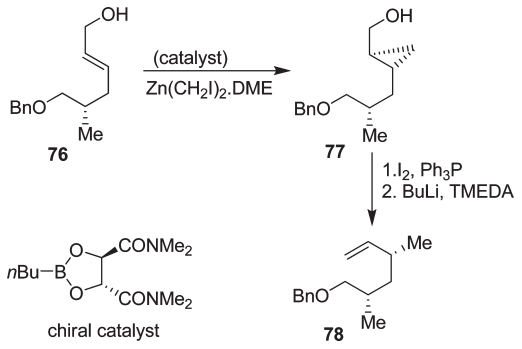

FIGURE 13. Stereoselective synthesis of polyketide fragment **78**.

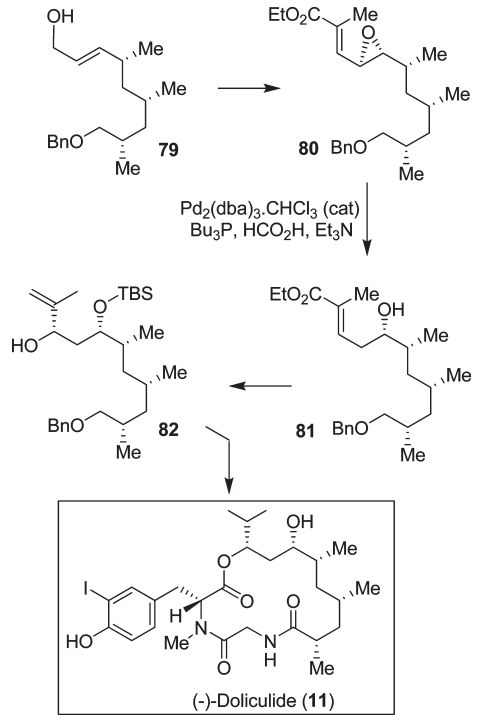

FIGURE 14. Synthesis of (−)-doliculide (**11**).

asymmetric epoxidation[45] and regioselective opening of the epoxide as the key steps. The regioselective epoxide opening of **80** using a catalytic amount of $Pd_2(dba)_3 \cdot CHCl_3$ provided *anti*-alcohol **81**, which was further converted to polyketide unit **82** and then to doliculide (**11**).[18]

Using synthetic doliculide, we have investigated its biological mechanism of action. It was found that doliculide arrested cells at the G_2/M phase of the cell cycle by interfering with normal actin assembly.[59] Furthermore, we found that doliculide, like jasplakinolide (**21**), enhanced the assembly of purified actin and inhibited the binding of FITC[2]-labeled phalloidin to actin polymer. Treatment of cells with doliculide resulted in the arrest at cytokinesis and caused major rearrangement of intracellular F-actin.[59] Structural similarities of doliculide and jasplakinolide led us to suggest that both compounds bind to the same site on F-actin. This finding prompted us to get involved in the synthesis of jasplakinolide (**21**)[28] and provided us an opportunity to design novel doliculide and jasplakinolide-based molecular probes.

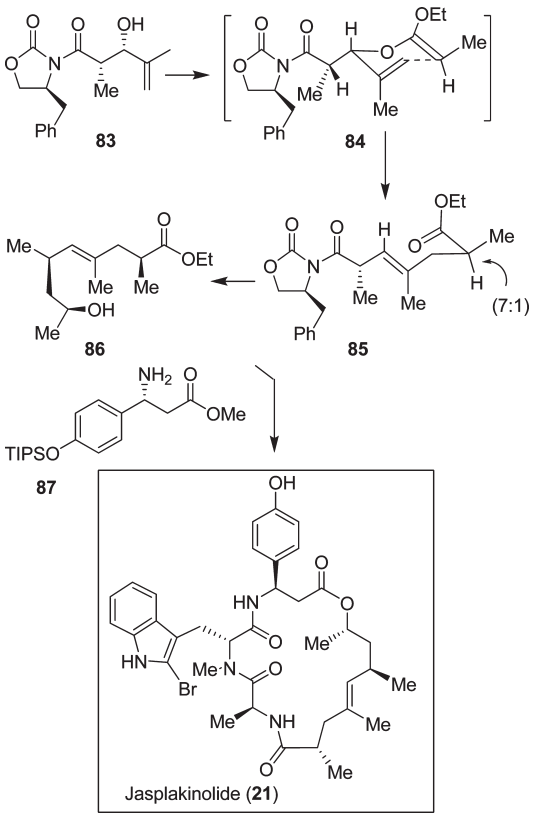

FIGURE 15. Synthesis of jasplakinolide (**21**).

Jasplakinolide (**21**) has shown good potency against numerous human solid tumor types in cell culture assays. As mentioned, its mode of action involves stabilization of actin filaments by binding to F-actin similar to phalloidin.[60] The clinical potential of jasplakinolide was further investigated by the National Cancer Institute. However, studies were terminated because of toxicity issues.[61] Chemical and biological investigations of jasplakinolide, and its analogues, remain an extremely active area of research. We have devised a practical synthesis of jasplakinolide that has enabled us to prepare a number of structural variants.[28] As shown in Figure 15, the polyketide segment of **21** was first constructed by a diastereoselective aldol reaction that provided **83**, followed by an ortho-ester-promoted Claisen rearrangement to form the γ,δ-unsaturated ester **85** in a 7:1 mixture of diastereomers. It was then converted to alcohol **86**. The β-amino acid segment **87** was synthesized using an asymmetric enolate addition to a chiral sulfinimine derivative developed by David and co-workers.[62] Strategic assembly of the various segments led to the synthesis of jasplakinolide (**21**).[28] This synthesis enabled us to probe the importance of various substituents, improve potency, and reduce complexity. As shown in Figure 16, two less complex jasplakinolide analogues have shown comparable potency (IC_{50}) to jasplakinolide, when assayed against CA46 Burkitt lymphoma human cell lines.[63] Analogue **88** (IC_{50} = 20 nM) allowed us to replace the metabolically susceptible phenolic OH with OMe. In analogue **89**, we have eliminated the C_2-methyl chiral center, and the resulting analogue maintained potency (IC_{50} = 10 nM).

Our interest in the synthesis of laulimalide (**12**) began in 1997, because of its intriguing structural features as well as its

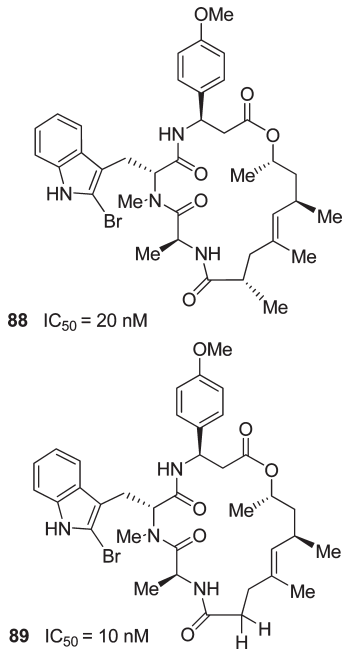

FIGURE 16. Potent analogs of jasplakinolide.

impressive cytotoxicity against KB cells (IC_{50} = 15 ng/mL) and many other NCI cell lines with IC_{50} values ranging from 10 to 50 ng/mL.[64] The biological mechanism of action of laulimalide was not known until 1999, when Susan Mooberry and co-workers first reported that, like paclitaxel, laulimalide stabilizes microtubule assembly.[65] Laulimalide's natural abundance is limited, it is unstable, and it readily converts to the significantly less potent isolaulimalide. Laulimalide contains nine chiral centers and appears to have similarities to the epothilones. Therefore, it was expected that, like epothilone, laulimalide may bind to a similar site as paclitaxel on β-tubulin. The report of Mooberry and co-workers[65] motivated our work on this molecule, and within a year, we were able to complete the first total synthesis of laulimalide.[19] Most importantly, our synthesis enabled us to carry out a number of important biological studies with synthetic laulimalide.

Our convergent synthesis utilized Grubb's olefin metathesis to construct both dihydropyran rings of laulimalide. As shown in Figure 17, ring-closing olefin metathesis of **90** followed by a highly diastereoselective anomeric alkylation and further standard synthetic transformations provided iodide **91**. The C_{13}-methylene unit and C_{15}-alcohol were introduced by a novel protocol developed by us.[19] As shown, alkylation of **92** with iodide **91** provided sulfone **93**. It was converted to **94** in a three-step sequence involving (1) reduction by Red-Al, (2) formation of the corresponding dibenzoate, and (3) Na−Hg reduction to provide **94** in 72% yield.

The C_{17}−C_{28} fragment synthesis was accomplished by the reaction of **95**-derived anion and aldehyde **96** to provide the corresponding alkyne derivative (Figure 18). The resulting product was converted to sulfone **97** (Figure 18). Julia olefination of **94**-derived aldehyde and sulfone **97** furnished *trans*-olefin **98** as the major product (3.4:1 *trans*/*cis* mixture). It was initially converted to laulimalide (**12**) by a Horner−Emmons-mediated macrolactonization as the key step.[19] An alternative synthesis of laulimalide was carried out in which

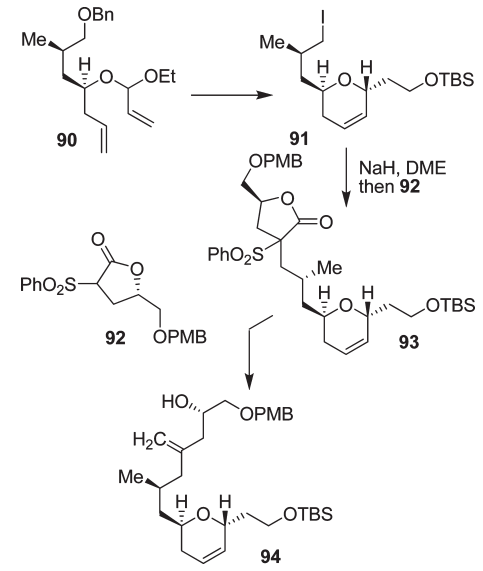

FIGURE 17. Synthesis of C_3−C_{16} segment of laulimalide (**12**).

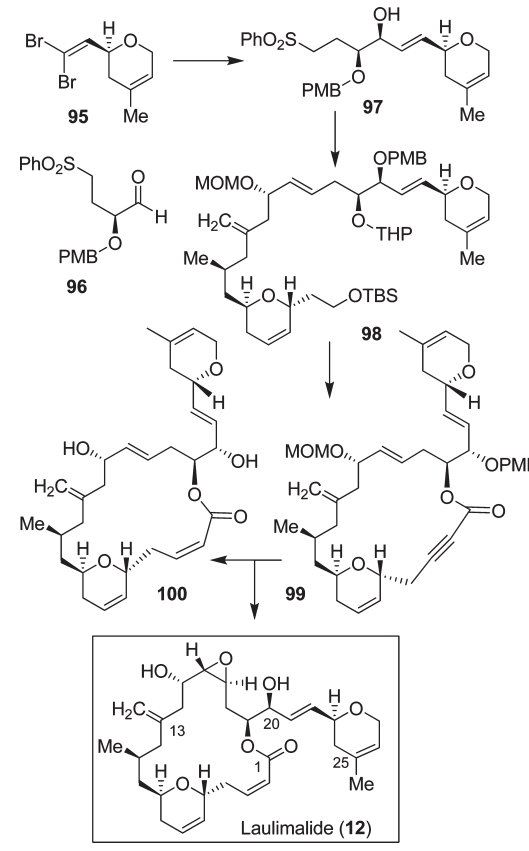

FIGURE 18. Synthesis of laulimalide (**12**).

the C_2−C_3 *cis*-olefin was installed selectively. As shown, alcohol **98** was converted to lactone **99**, which upon hydrogenation over Lindlar's catalyst provided the corresponding *cis*-macrolactone as a single isomer. The *cis*-lactone was converted to laulimalide (**12**).[19,66]

Using our synthetic laulimalide, Dr. Hamel at the NCI has shown that laulimalide, while as active as paclitaxel in promoting the assembly of cold-stable microtubules, was

unable to inhibit the binding of radiolabeled paclitaxel or a fluorescent paclitaxel derivative to tubulin. Laulimalide has shown potent activity against cell lines resistant to paclitaxel and epothilones A and B on the basis of mutations on M40 human-tubulin gene.[67] Furthermore, laulimalide was able to enhance tubulin assembly synergistically with paclitaxel.[68] Taken together, laulimalide appeared to be the first example of a ligand for an unknown drug-binding site on tubulin. Our biological evaluation of synthetic intermediates and limited structural variants identified desoxylaulimalide (**100**, $IC_{50} = 25 \pm 5\,\mu M$; laulimalide (**12**), $IC_{50} = 17 \pm 3\,\mu M$) to be nearly as potent as laulimalide.[67] Since our discovery that laulimalide stabilizes microtubules by binding to tubulin at a different site from paclitaxel, further exploration of its chemistry and biology intensified.[69] Unlike paclitaxel, laulimalide is not a substrate for P-glycoprotein and also has shown potent activity against paclitaxel-resistant cell lines.[67] Our synthesis and subsequent biological studies demonstrated the clinical potential of laulimalide. Since laulimalide's natural abundance is extremely limited, the design of more potent and less complex laulimalide-based synthetic derivatives is warranted.

Interestingly, at about the same time, when we were concluding our synthesis of laulimalide, Northcote and co-workers reported the isolation and structure elucidation of peloruside A (**24**), a novel 16-membered macrolide isolated from a New Zealand marine sponge.[70] It displayed potent cytotoxicity against P388 murine leukemia cells with an IC_{50} value of 10 ng/mL. Since its isolation, Miller and co-workers then reported very intriguing properties of peloruside A. It turned out peloruside A is a microtubule-stabilizing agent that arrests cells in the G2-M phase of the cell cycle.[71] Furthermore, peloruside A binds to a nontaxoid site on tubulin and has shown a synergistic effect with paclitaxel.[72] Peloruside A also has a very low natural abundance, and its structural complexity and clinical potential attracted our attention to its synthesis and subsequent biological studies.

Our synthesis of peloruside A includes the development of a new diastereoselective reductive aldol reaction that assembled the C_1-C_{10} and $C_{11}-C_{24}$ segments.[31] As shown in Figure 19, isopropylidene-D-threitol **101** was efficiently converted to homoallylic alcohol **102** using Brown's asymmetric allylation[73] as one of the key steps. Alcohol **102** was converted to α,β-unsaturated ester **103**. Sharpless' asymmetric dihydroxylation[74] introduced the C_7 and C_8-diol stereochemistry. The resulting diol was converted to enone **104**. The $C_{11}-C_{20}$ fragment **106** was synthesized from chiral imide **105**. Asymmetric alkylation established the C_{18} stereocenter, and successive asymmetric allylboration introduced C_{13} and C_{15} stereocenters in **106**. A one-pot L-Selectride-mediated reduction of **104** followed by aldol reaction with aldehyde **106** afforded **107** as a 4:1 mixture of diastereomers in 92% yield (Figure 20). Yamaguchi macrocyclization of the resulting seco acid furnished macrolactone **108**, which was ultimately converted to peloruside A.[31]

During the course of our synthesis of peloruside A, Northcote and co-workers isolated a compound from *M. hentscheli,* named peloruside B (**25**).[32] It is the 3-des-*O*-methyl variant of peloruside A and was isolated in submilligram quantities. Peloruside B's activity is comparable to that of peloruside A as it arrests cells in the G_2/M phase of mitosis. The structure

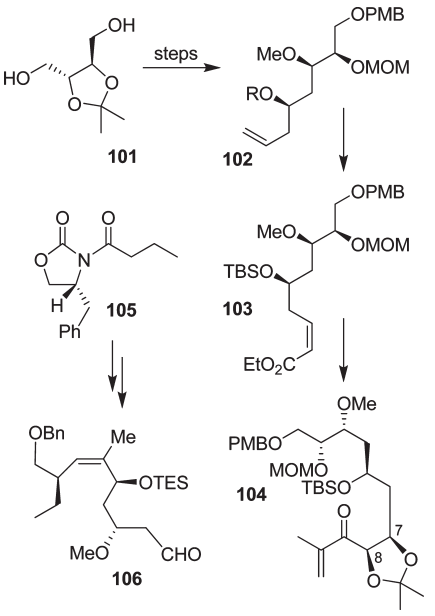

FIGURE 19. Synthesis of peloruside A subunits **104** and **106**.

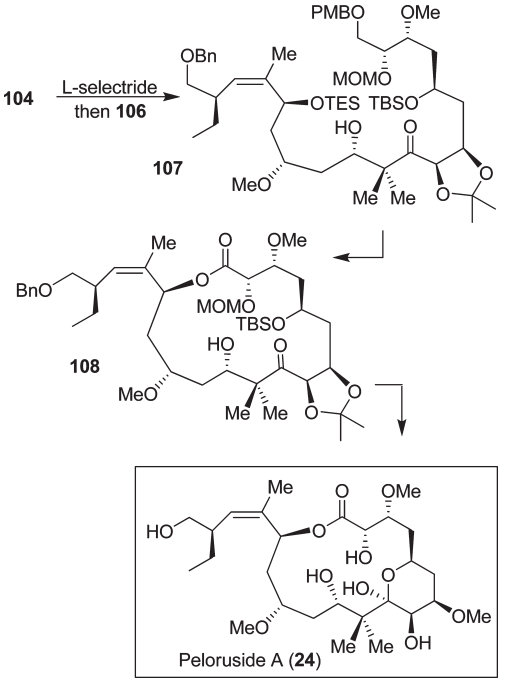

FIGURE 20. Synthesis of peloruside A (**24**).

of peloruside B was confirmed with our total synthesis and comparison of its bioactivity in a trans-Pacific collaborative effort.[32] Our synthesis of peloruside B followed a similar strategy as peloruside A.[31] As shown in Figure 21, the synthesis started with diethyl D-tartrate-derived bis-MOM derivative **109**, which was converted to enone **110**. A reductive aldol strategy described previously[31] assembled the key fragments, providing **111** as the major diastereomer (6.5:1 mixture) in 66% yield. This was then converted to peloruside B.[32] The structure of natural peloruside B was confirmed by comparison of the 1D and 2D NMR data of synthetic and natural peloruside B. Furthermore, on the basis of comparison of the

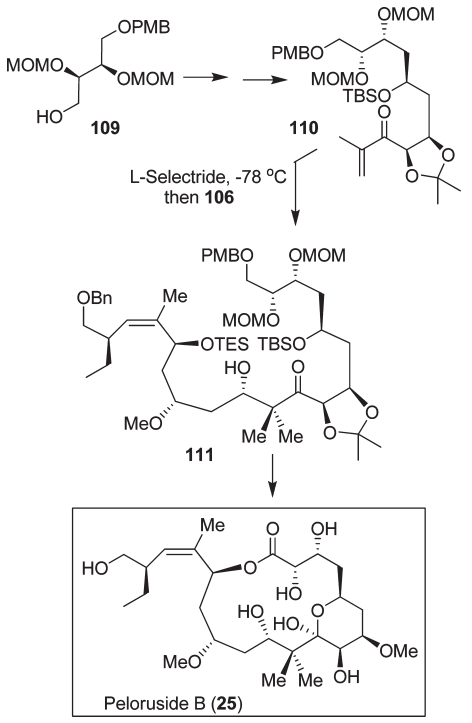

FIGURE 21. Synthesis and structural confirmation of peloruside B (**25**).

bioactivity of synthetic and natural peloruside B, we were able to establish the absolute configuration of peloruside B. Following the synthesis of pelorusides A and B, we have synthesized a number of structural variants of peloruside A and prepared tritiated peloruside A for mechanistic studies. As mentioned above, like laulimalide, pelorusides A and B bind to tubulin at a different site than paclitaxel. Our investigation, in collaboration with Dr. Ernest Hamel, on the drug-binding site of peloruside A will be reported in due course.[75]

Our syntheses of Al-77-B (**13**)[20] and amphidinolide T1 (**15**)[22] demonstrated the scope and utility of our ester-derived titanium enolate-based asymmetric *syn*- and *anti*-aldol reactions.[76] Al-77-B is a medicinally significant target.[77] It has exhibited important gastroprotective properties. Because of its clinical potential, it drew considerable interests in synthesis and biological studies.[78a,b]

Our synthesis utilized a highly diastereoselective aldol reaction to install four of the five stereocenters of Al-77-B.[20] The dihydroisocoumarin skeleton was constructed by a thermal Diels–Alder reaction as shown in Figure 22. Aldolate **112** was obtained in 90% yield as a 19:1 mixture (*anti*/*syn*).[20] Curtius rearrangement, protection as an isopropylidene derivative followed by treatment with *n*-BuLi/TMEDA and methyl chloroformate provided **113**. Diels–Alder reaction of **113** with methoxycyclohexadiene proceeded smoothly, and the resulting product was cyclized to isochromanone **114** in 74% yield, over two steps. The hydroxy amino acid fragment **115** was also assembled by a *syn*-aldol reaction as the key step. Coupling of **114** and **115** provided amide **116**, which was converted to Al-77-B.[20]

Kobayashi and co-workers[79] isolated a new class of natural products named the amphidinolides, which have shown significant antitumor properties against a variety of NCI tumor

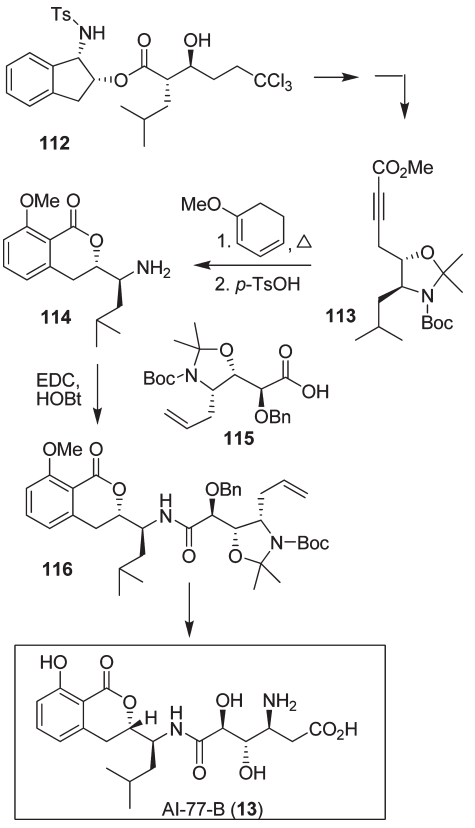

FIGURE 22. Synthesis of Al-77-B (**13**).

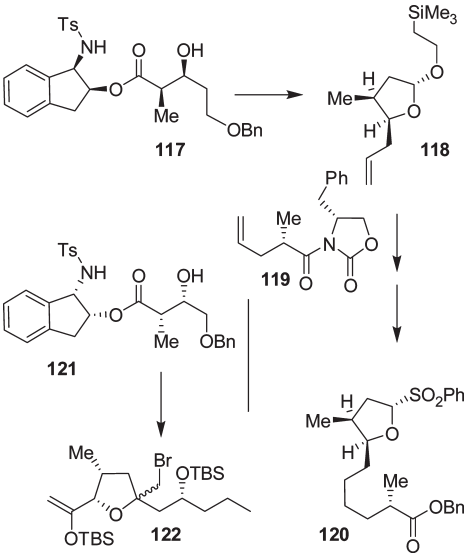

FIGURE 23. Synthesis of sulfone **120** and bromo ether **122**.

cell lines. Amphidinolides are extremely scarce, and subsequent biological studies have been limited. In many cases, structural assignment was hampered due to a lack of natural abundance.[79] We carried out the first syntheses of amphidinolide T1, amphidinolide W, and more recently, iriomoteolides **28** and **29** that were isolated from *Amphidinium* sp.

Our synthesis of amphidinolide T1 utilized a highly diastereoselective ester-derived Ti-enolate aldol reaction. As outlined in Figure 23, aldol product **117** was obtained as a

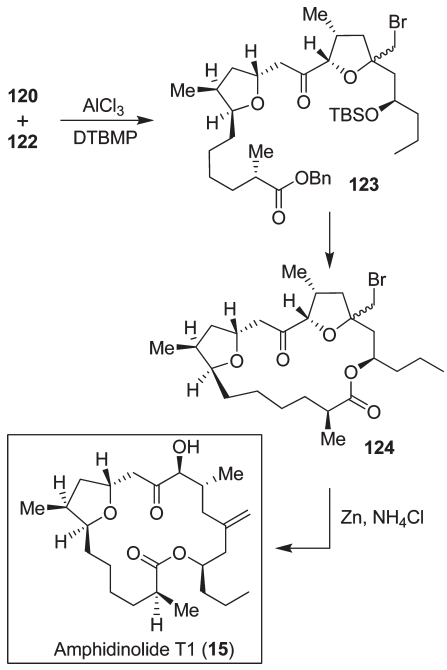

FIGURE 24. Synthesis of amphidinolide T1 (**15**).

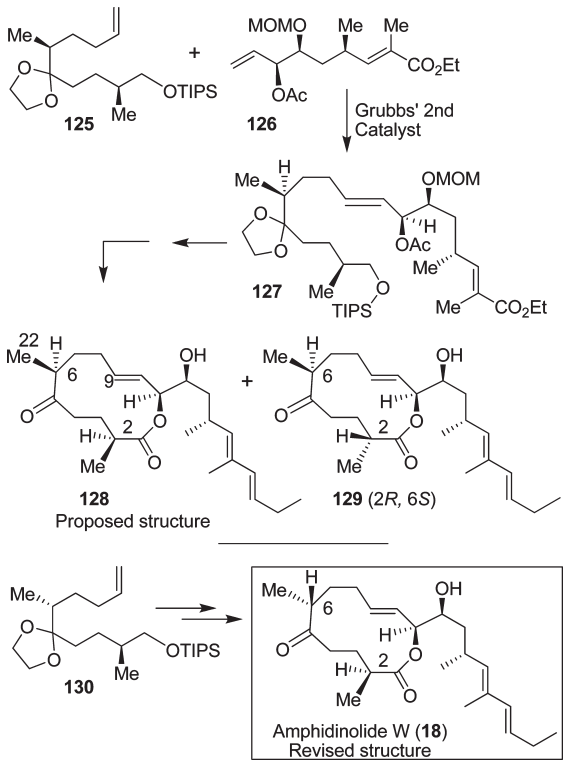

FIGURE 25. Synthesis and structural revision of amphidinolide W (**18**).

single diastereomer in 90% yield. It was converted to tetrahydrofuran derivative **118**. Cross-metathesis of **118** with oxazolidinone derivative **119** was carried out using Grubb's second-generation catalyst.[80] The resulting product was converted to sulfone **120**. Aldolate **121** was also obtained as a single product in 95% yield. It was transformed into bromotetrahydrofuran **122**. A highly stereoselective oxocarbenium ion-mediated alkylation of **120** with **122** provided **123** as a single product in 73% yield (Figure 24). It was converted to macrolactone **124**. A reductive opening of bromo ether **124** with Zn/NH_4Cl provided synthetic amphidinolide T1.

We also carried out the first synthesis and revision of the structure of amphidinolide W (**18**).[25] As depicted in Figure 25, the C_1-C_9 segment **125** was synthesized by asymmetric alkylation and Horner–Emmons reaction as the key steps. The $C_{10}-C_{20}$ segment **126** was prepared by asymmetric dihydroxylation as the key step. Cross-metathesis[80] of **125** with **126** provided **127**. Macrolactonization of the **127**-derived seco acid provided a 3:1 mixture of macrolactones. These were converted to the proposed structure of amphidinolide **128** and its epimer **129**. However, neither structure matched with the reported spectral data of the natural product. Our comparison of NMRs of the synthetic and natural amphidinolide W revealed discrepancies of chemical shifts at the C_6 stereocenter. On the basis of this observation, we carried out the synthesis of the C_6 epimeric seco acid starting from the C_1-C_9, segment **130**, which upon macrocyclization afforded the corresponding macrolactone as a 1:1 mixture. The removal of protecting groups from the C-6 epimer provided amphidinolide W (**18**), which was in complete agreement with the reported spectral data and optical rotation of natural amphidinolide W.[25]

We embarked on the synthesis of (−)-lasonolide A (**22**) due to its potent antitumor properties and a lack of knowledge of its biological mechanism of action. Lasonolide A's natural abundance is low, and no structure–activity studies have been reported. Lasonolides are a group of natural products isolated from a Caribbean marine sponge. Among this family, lasonolide A has shown the most potent cytotoxicity with IC_{50} values of 8.6 and 89 nM against A-549 human lung carcinoma and panc-1 human pancreatic carcinoma, respectively. Lasonolide A contains nine chiral centers with two highly functionalized tetrahydropyran rings. As shown in Figure 26, both tetrahydropyran rings have been constructed stereoselectively. Intramolecular 1,3-dipolar cycloaddition of **131** provided bicyclic isooxazoline **132**, which allowed for the construction of the pyran ring as well as the quaternary stereocenter in **22**. It was converted to isopropylidene derivative **133**.

An asymmetric hetero-Diels-Alder reaction of diene **134** and silyloxyacetaldehyde using Jacobsen's catalyst **135** afforded **136** with three chiral centers in high optical purity (94% ee). This was converted to aldehyde **137**. Julia olefination of **137** with sulfone **133** afforded *E*-olefin **138** (Figure 27). Macrolactone **139** was prepared by intramolecular Horner–Emmons reaction. This was converted to lasonolide A (**22**).[29] Using synthetic lasonolide A, we have investigated the biological mechanism of action in collaboration with Dr. Yves Pommier of the National Cancer Institute. Our studies revealed that lasonolide A unusually induces premature chromosome condensation.[81] This finding may lead to the treatment of many disorders.[81]

The discovery of platensimycin (**19**) and platencin (**20**) as inhibitors of bacterial β-ketoacyl synthase (FabF), by Merck researchers, grasped the attention of chemists and biologists around the world.[82] Since the discovery of penicillins in the 1940s, isolation and characterization of novel antibiotic natural products have been limited. Both platensimycin and platencin exhibited a broad range of activity against Gram-positive organisms, good *in vivo* efficacy, and no

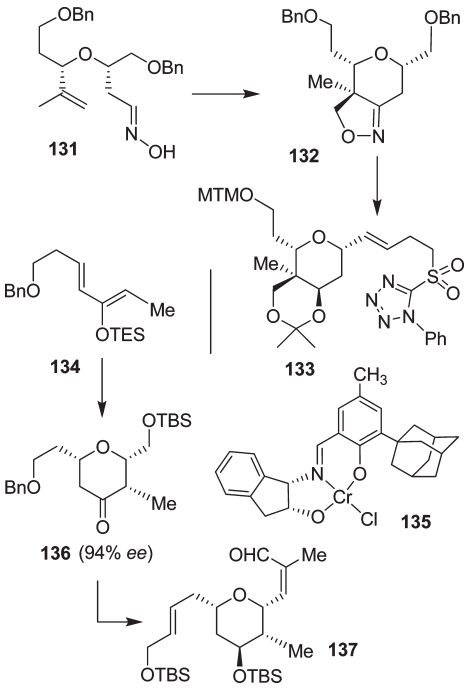

FIGURE 26. Synthesis of tetrahydropyran derivatives.

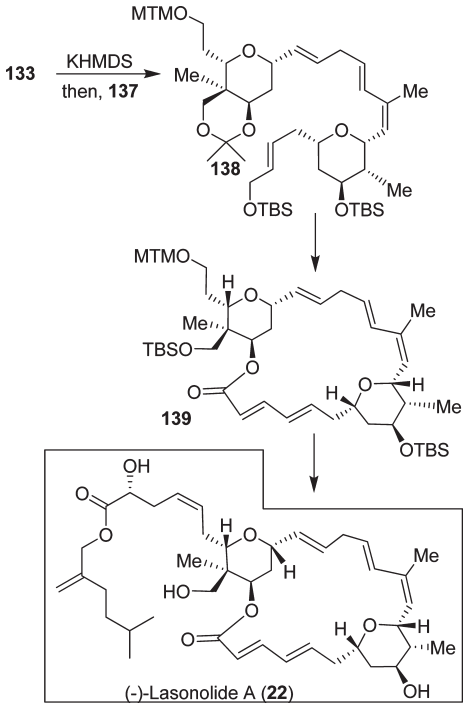

FIGURE 27. Synthesis of (−)-lasonolide A (**22**).

observed toxicity in mice.[82] However, both these natural products showed very poor pharmacokinetic properties and could not be used as drugs.[83] Therefore, structural changes are necessary for these natural product leads, which have become a subject of great synthetic interest.[84]

Our synthesis of the platensimycin core is unique in the sense that we planned to construct it using an intramolecular Diels−Alder reaction.[26] As shown in Figure 28, (+)-carvone **140** was converted to bicyclic ketone **141**. Horner−Emmons

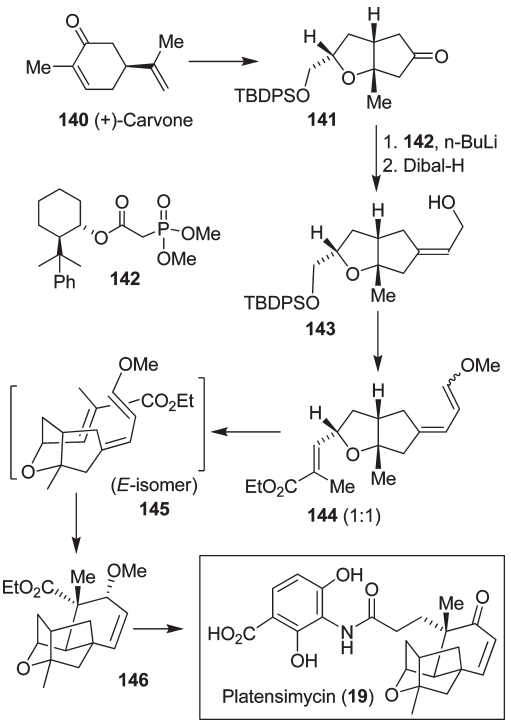

FIGURE 28. Synthesis of platensimycin (**19**).

olefination of **141** with chiral phosphonoacetate **142** was utilized to obtain *E*-olefin **143** selectively (*E*/*Z* ratio 4.5:1). Triethyl phosphonoacetate in comparison provided **143** as a 1.5:1 *E*/*Z* olefin mixture. Olefin **143** was converted to triene **144**, the Diels−Alder precursor. Thermal Diels−Alder reaction in a sealed tube with chlorobenzene as solvent in the presence of 2,6-di-*tert*-butyl-4-methylphenol (BHT) as a radical inhibitor provided **146**. Only the *E*-isomer **145** underwent cyclization, and the *Z*-isomer was recovered and recycled after isomerization. Diels−Alder product **146** was obtained in 44% overall yield from **144**. This was converted to platensimycin (**19**).[26]

We have carried out a concise formal synthesis of platencin using a symmetry-based approach.[27] As shown in Figure 29, synthesis of enone **148** was achieved from commercially available cyclohexenone **147**. Michael reaction of **148** with catalytic *t*-BuOK in THF at reflux afforded symmetric diketone **149**. Selective monoreduction of diketone by LiAl(O-*t*-Bu)$_3$H provided the corresponding alcohol (7:1 mixture, 83% yield). This was converted to iodide **150**. Radical cyclization of **150** with *n*-Bu$_3$SnH in the presence of AlBN resulted in platencin core **151**, which was converted to enone **152**. This was previously converted to platencin.[85] Our synthesis provided a quick and efficient access to the platencin core structure.[27]

Iriomoteolide 1a (**28**) attracted our attention because of its structural resemblance to laulimalide (**12**) and peloruside A (**24**). Iriomoteolide 1a (**28**) has shown exceedingly potent cytotoxicity against human B lymphocyte DG-75 cells with IC$_{50}$ values of 2 ng/mL.[86] The biological mechanism of action of iriomoteolide 1a is presently unknown. Iriomoteolide 1a has been isolated in minute quantities, and the structures of iriomoteolides 1a and 1b were elucidated by spectroscopic studies. Our preliminary work leading to the synthesis of the proposed structures of both iriomoteolide 1a

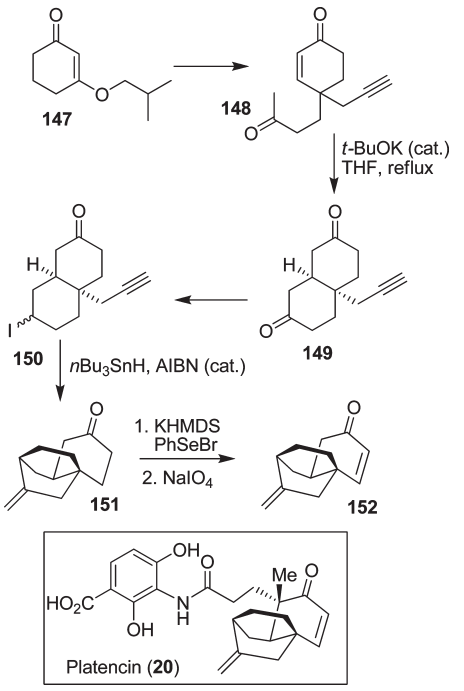

FIGURE 29. Formal synthesis of platencin (**20**).

(**28**) and iriomoteolide 1b (**29**) suggested that both structures were assigned incorrectly.[35]

Our convergent synthesis of the proposed structures of iriomoteolides is shown in Figures 30 and 31. A Sakurai reaction of allyl silane **153** with aldehyde **154** provided **155** after oxidation of the sulfide to sulfone. This was converted to aldehyde **156** utilizing a Julia−Kocienski olefination as the key step. Optically active alcohol **157** was prepared using Brown's asymmetric crotylboration.[87] This was converted to sulfone **158**. The key Julia olefination of **156** with **158** provided **159** in 70% yield. Yamaguchi macrolactonization of **159**-derived seco acid furnished macrolactone **160**. It was further transformed into the proposed structures of iriomoteolide 1a (**28**) and iriomoteolide 1b (**29**).[35] Our detailed spectroscopic studies of the structures of **28** and **29** provided a number of discrepancies at some specific carbon centers of the reported NMR spectra. This information is currently being used for the structural assignment of these natural products. Our current investigation is focused on both structural and biological studies of iriomoteolides.

Development of Asymmetric Methodologies

In the context of our syntheses of natural and unnatural bioactive molecules, we have developed a variety of asymmetric methodologies. These include asymmetric *anti*- and *syn*-aldol reactions, asymmetric multicomponent reactions, and asymmetric reductive aldol reactions. Asymmetric aldol reactions have been a significant development in organic synthesis.[88] A number of practical and reliable technologies have evolved over the years, particularly for the asymmetric generation of *syn*-aldol products. These asymmetric processes have been extensively used in the synthesis of complex bioactive molecules with multiple stereocenters. This subject has been an active area of investigation for nearly three decades.[88] While asymmetric *syn*-aldols, most notably Evans' chiral oxazolidinone-based aldol additions,[38] are widely used, the corresponding *anti*-aldol

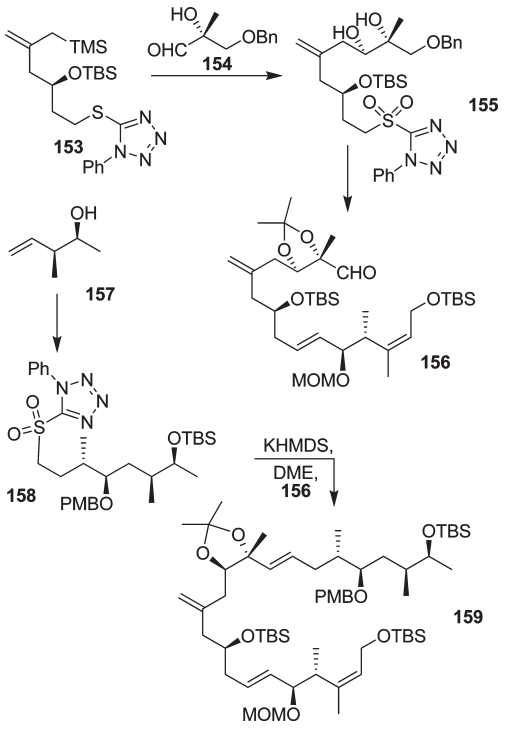

FIGURE 30. Synthesis of **159** by double Julia olefinations.

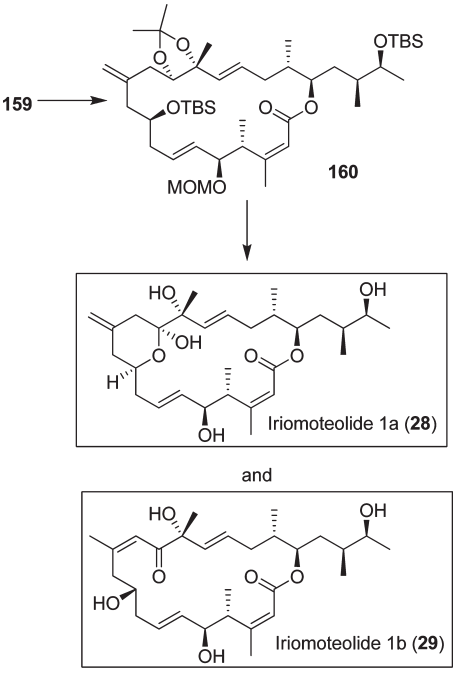

FIGURE 31. Synthesis of the proposed structures of iriomoteolides 1a (**28**) and 1b (**29**).

reactions are used less frequently due to a lack of practical asymmetric *anti*-aldol reactions.[88]

Development of Asymmetric *anti*-Aldol Reactions

We have developed highly diastereoselective ester-derived titanium enolate-based *anti*-aldol reactions using conformationally constrained cyclic amino alcohol-derived chiral

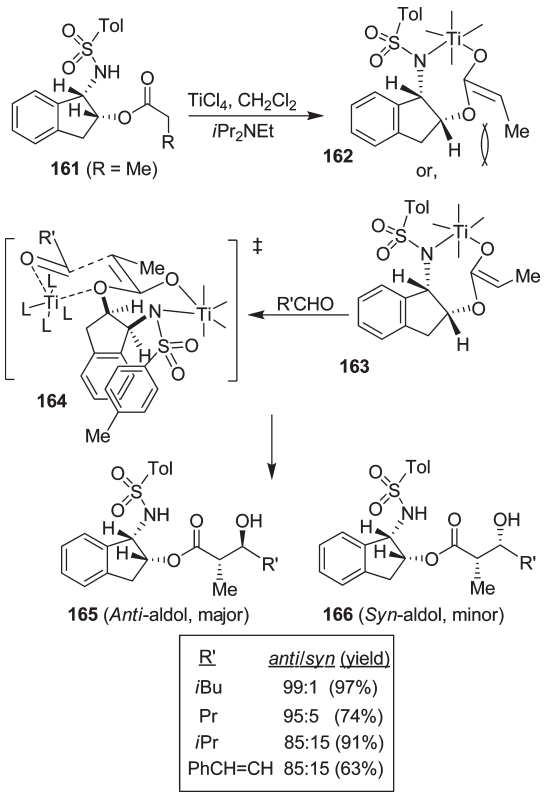

R'	*anti*/*syn* (yield)
*i*Bu	99:1 (97%)
Pr	95:5 (74%)
*i*Pr	85:15 (91%)
PhCH=CH	85:15 (63%)

FIGURE 32. Ti-enolate-based asymmetric *anti*-aldol reaction.

sulfonamide **161**.[89] Optically active (1*S*,2*R*) and (1*R*,2*S*)-1-amino-2-indanols are readily available commercially as well as through practical synthesis, enabling the synthesis of both enantiomers of the *anti*-aldol product. The propionate derivative **161** was readily prepared by tosylation of 1-amino-2-indanol followed by *O*-acylation with propionyl chloride (Figure 32). The titanium enolate of **161** was readily formed by treatment with $TiCl_4$ and diisopropylethylamine at 0 °C in CH_2Cl_2 for 1 h.[89] The alkyl ester alone cannot be enolized effectively with $TiCl_4$ and a base.[91] However, smooth enolization of **161** was possible presumably due to internal chelation with the sulfonamide group as shown in **163**. This type of enolate formation was first shown by Xiang et al.[92]

The ^{1}H NMR analysis revealed the presence of a single enolate. The *Z*-enolate **163** is preferred over **162** due to the minimization of the 1,3-allylic strain between the methyl group and the indanol auxiliary. Also, ^{1}H NMR spectra showed the disappearance of the sulfonamide hydrogen, which supported the formation of the cyclic enolate shown. Treatment of the resulting enolate directly with isovaleraldehyde provided no aldol addition product. However, reaction of the enolate with isovaleraldehyde precomplexed with $TiCl_4$, provided the *anti*-aldol product **165** (R = *i*-Bu) as a single isomer (by HPLC and NMR analysis). Reactions with a variety of monodentate aldehydes also provided the *anti*-aldols with excellent diastereoselectivity and isolated yields. It should be noted that among four possible diastereomers, only one *anti*-aldol (**165**) and one *syn*-aldol (**166**) product were observed in this reaction.[89]

The stereochemical outcome of the *anti*-addition could be rationalized by using the Zimmerman−Traxler-type transition-state model **164**.[93] The model is based upon the assumptions that the titanium enolate geometry is *Z*, the titanium enolate is a seven-membered metallocycle with a pseudo-chairlike conformation and a second Ti is chelated to the indanyloxy group as well as to the aldehyde carbonyl in a six-membered chairlike transition state. The model explains our observed diastereoselectivity.[89] Our subsequent structure−selectivity studies revealed that ring, substitution, and stereochemistry are all critical to the observed high *anti*-aldol diastereoselectivity.[88] The reaction of the corresponding *N*-mesylamine indanol with isovaleraldehyde provided a 70:30 mixture of *anti*/*syn* diastereomers. This result suggested that a possible π-stacking interaction between the two aromatic rings may have provided the stabilization of the enolate conformation shown in **164**.

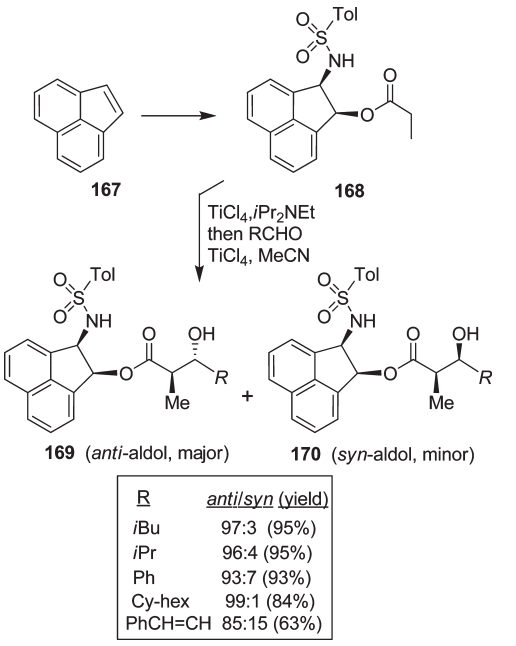

R	*anti*/*syn* (yield)
*i*Bu	97:3 (95%)
*i*Pr	96:4 (95%)
Ph	93:7 (93%)
Cy-hex	99:1 (84%)
PhCH=CH	85:15 (63%)

FIGURE 33. *cis*-2-Amino-1-acenaphthenol-based *anti*-aldol reactions.

Based upon the results, we then speculated that the planarity of the acenaphthene ring may further enhance secondary-orbital interactions with the arylsulfonamide functionality. We have developed effective syntheses of both enantiomers of *cis*-2-amino-1-acenaphthenol in high enantiomeric excess (>98% ee) employing lipase-catalyzed enzymatic resolution as a key step.[94] The aldol reaction of propionate ester **168** (Figure 33) with isovaleraldehyde however, provided a significant reduction in *anti*-diastereoselectivity. The use of various chelating additives led to an improvement in diastereoselectivity for **169**. It turned out that 2.2 equiv of acetonitrile provided a significant improvement of *anti*-diastereoselectivity as well as yield with a variety monodentate aldehydes.[94]

We investigated the effects of a variety of other additives. Both acetonitrile and *N*-methylpyrrolidinone (NMP) showed the best results with respect to *anti*-diastereoselectivity and isolated yields. These conditions were employed in the asymmetric aldol reaction of chloroacetate with a range of monodentate aldehydes. Both NMP and acetonitrile as additives provided the best results, affording consistently excellent *anti*-diastereoselectivity and yields. The chloroacetate aldol reaction provided access to acetate aldol products in high ee.[95]

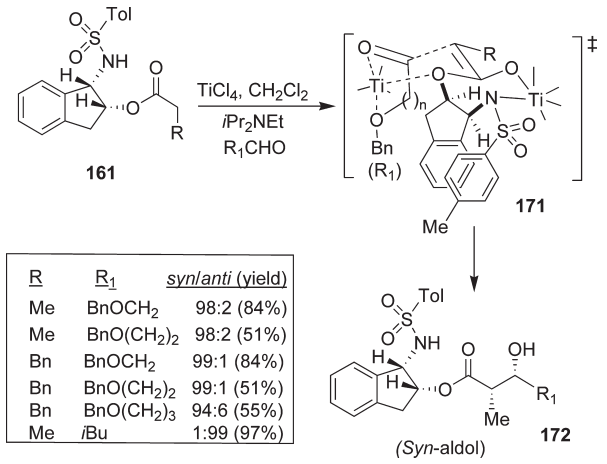

R	R_1	*syn*/*anti* (yield)
Me	$BnOCH_2$	98:2 (84%)
Me	$BnO(CH_2)_2$	98:2 (51%)
Bn	$BnOCH_2$	99:1 (84%)
Bn	$BnO(CH_2)_2$	99:1 (51%)
Bn	$BnO(CH_2)_3$	94:6 (55%)
Me	*i*Bu	1:99 (97%)

FIGURE 34. Development of the asymmetric *syn*-aldol reaction.

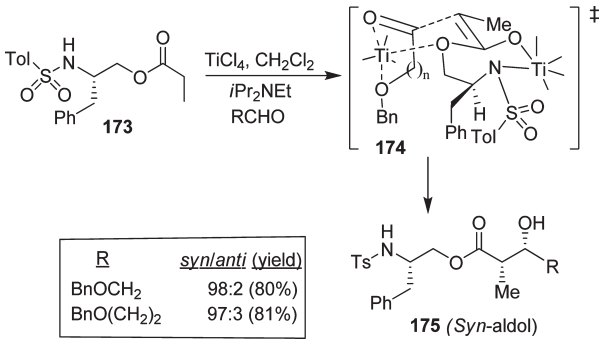

R	*syn*/*anti* (yield)
$BnOCH_2$	98:2 (80%)
$BnO(CH_2)_2$	97:3 (81%)

FIGURE 35. Phenylalaninol-based highly diastereoselective *syn*-aldol reactions.

Development of Asymmetric *syn*-Aldol Reactions

Based upon the proposed transition-state assembly for the *anti*-aldol reaction,[89] we postulated that a bidentate alkoxy-aldehyde would adopt a transition state like **171** (Figure 34) so that the ether oxygen could effectively donate its lone pair to the vacant d-orbital of titanium and the alkoxy aldehyde side chain will be oriented pseudoaxially, giving rise to *syn*-aldol product **172** selectively.[96] Indeed, reaction of benzyloxyacetaldehyde and benzyloxypropionaldehyde proceeded with excellent diastereoselectivity. The aldol reaction with benzyloxybutyraldehyde provided slightly reduced *syn*-diastereoselectivity (dr 94:6). Aldol reactions of chloroacetate with the bidentate aldehydes provided aldol products with high *syn*-diastereoselectivity and yields.[95]

Based upon our proposed highly chelated transition state, we further speculated that the α-chiral center on the indane ring may not be required for *syn*-diastereoselectivity with bidentate aldehydes. We therefore investigated amino acid-derived chiral sulfonamides. As shown in Figure 35, phenylalaninol-derived auxiliary **173** provided aldol product **175** with excellent *syn*-diastereoselectivity (dr 98:2) with alkoxy-aldehyde. We have also investigated double diastereodifferentiation using chiral bidentate aldehydes. In a matched case, (*R*)-2-benzyloxypropionaldehyde furnished the *syn*-diastereomer. However, the (*S*)-aldehyde provided an *anti*-aldol diastereomer.[97] The (*S*)-benzyloxypropionaldehyde was recovered in 40% yield with 94% ee.[97]

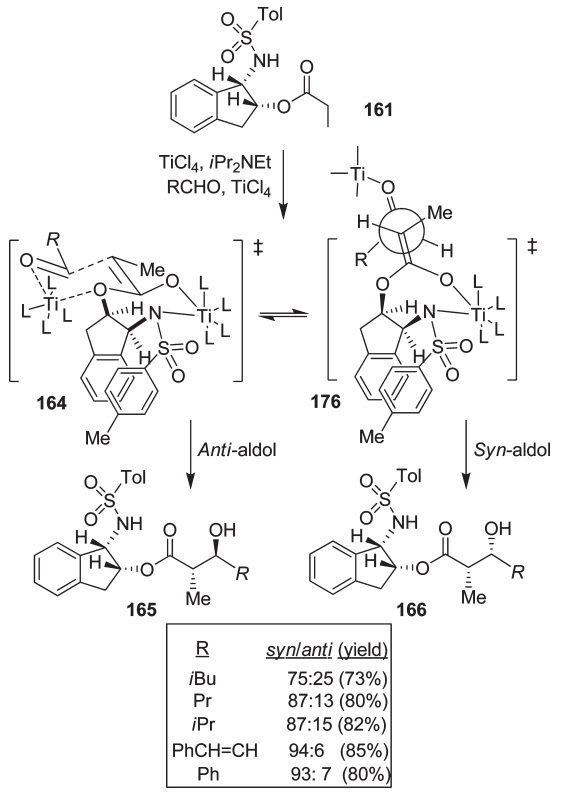

R	*syn*/*anti* (yield)
*i*Bu	75:25 (73%)
Pr	87:13 (80%)
*i*Pr	87:15 (82%)
PhCH=CH	94:6 (85%)
Ph	93: 7 (80%)

FIGURE 36. Development *syn*-aldol with monodentate aldehydes.

As mentioned previously, activation of monodentate aldehydes with $TiCl_4$ and other Lewis acids were necessary to observe *anti*-diastereoselectivity.[89] We have subsequently investigated the effect of increasing quantities of $TiCl_4$ on the *syn*/*anti* product ratio and reaction yields.[22b,97] Interestingly, when cinnamaldehyde was complexed with 3 equiv of $TiCl_4$, there was a dramatic reversal of diastereoselectivity. Reaction of **161** with 2 equiv of cinnamaldehyde, precomplexed with 5 equiv of $TiCl_4$, provided excellent yield (85%) and excellent *syn*-diastereoselectivity (dr 94:6). As shown in Figure 36, the generality of this reaction was examined with a variety of aldehydes. We rationalized the stereochemical outcome by using open-chain transition state model **176**, which is favored with excess equivalents of $TiCl_4$ and provides *syn*-aldol product diastereoselectivity.

These mechanism-based ester-derived Ti-enolate aldol additions, developed in our laboratory, were extensively utilized in the synthesis of numerous bioactive natural products as well as in the synthesis of the *bis*-THF ligand for darunavir[98] and peptidomimetic derivatives[99] for medicinal chemistry. One of the interesting features of the current asymmetric aldol reaction is that either *syn*- or *anti*-aldol product can be generated from the same chiral auxiliary with the appropriate choice of aldehyde and the stoichiometry of $TiCl_4$ used. Furthermore, the ready availability of both enantiomers of the *cis*-aminoindanol[90] provides an access to all possible *syn* and *anti*-aldols in optically active form.

Asymmetric Diels−Alder and Hetero-Diels−Alder reactions

We have demonstrated the usefulness of the *cis*-aminoindanol as a chiral auxiliary in a variety of transformations including Diels−Alder reactions, aldol reactions, and asymmetric

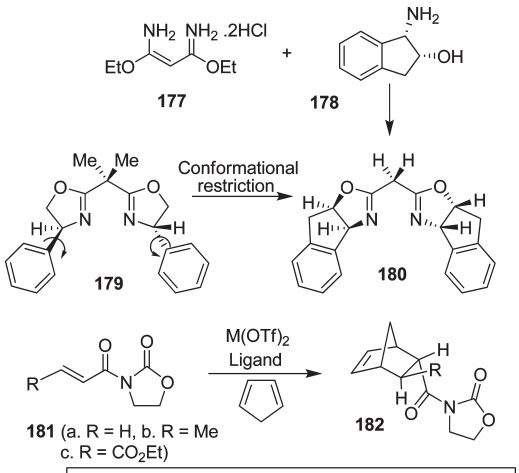

Dienophile	$M(OTf)_2$ (mol%)	*endo:exo*	yield	% *ee*
181a	$Cu(OTf)_2$ (4)	>99:1	90%	99 (*R*)
181a	$Mg(OTf)_2$ (100)	98:2	81%	61 (*S*)
181b	$Cu(OTf)_2$ (10)	90:10	77%	84 (*R*)
181b	$Mg(OTf)_2$ (10)	92:8	76%	55 (*S*)
181c	$Cu(OTf)_2$ (10)	93:7	75%	94 (*S*)

FIGURE 37. Chiral bis-oxazoline-metal-catalyzed Diels–Alder reactions.

reductions.[90] Subsequently, we have investigated *cis*-aminoindanol-derived bis(oxazoline)-metal-catalyzed asymmetric reactions.[100] The C_2-symmetric chiral bis(oxazoline) ligands have now been developed as privileged ligands for a variety of asymmetric transformations.[101] Early investigation in this area involved bis(oxazoline)-Cu(II)-catalyzed asymmetric cyclopropanation by Masamune et al.,[102] asymmetric Diels–Alder reactions with Phe-Box-Fe(III) and Phe-Box-Mg(II) by Corey,[103] and *t*-Box-Cu(II)-catalyzed reactions by Evans.[104] In an effort to improve Phe-Box-Cu(II)-catalyzed Diels–Alder reactions, we speculated that the *cis*-aminoindanol-derived bis(oxazoline) may well serve as a conformationally constrained alternative to the Phe-Box ligand. In this context, we first prepared aminoindanol-derived bis(oxazoline) ligands **180** and *ent*-**180** by condensation of the imidate salt **177** with optically active aminoindanol **178** as shown in Figure 37.[105] We have prepared a variety of metal–bis(oxazoline) complexes as catalysts for asymmetric Diels–Alder and hetero-Diels–Alder reactions. As shown, Cu(II)-catalyzed reactions with acryloyl-*N*-oxazolidinone proceeded with excellent *endo*/*exo* selectivity as well as *endo*-enantioselectivity (up to 99% ee), in contrast to Phe-Box-Cu(II)-catalyzed reactions (30% ee).[105] On the basis of this result, a variety of *N*-acyloxazolidinones were surveyed, and INDA-Box-Cu(II) showed consistently good to excellent enantioselectivity with 10 mol % ligand–metal complexes.[105]

Furthermore, we have investigated cationic aqua complexes derived from INDA-Box and $Cu(ClO_4)_2 \cdot 6H_2O$ and $Ni(ClO_4)_2 \cdot 6H_2O$, which provided excellent yield and enantioselectivity (up to 98% ee).[106] Interestingly, we have observed a reversal of enantioselectivity with Mg(II)-catalyzed reactions (55–65% ee).[105,106] These results were rationalized using a square planar model of the Cu(II)–ligand complex **183** and a *S-cis* conformation of the dienophile as shown in Figure 38. As can be seen, an *endo-Si*-face attack is favored. For the Mg(II)-catalyzed reaction, we assumed a tetrahedral Mg(II) geometry (**184**) as proposed by Corey and Ishihara.[103] An *endo-Re* face attack of cyclopentadiene explains the reversal of selectivity caused by

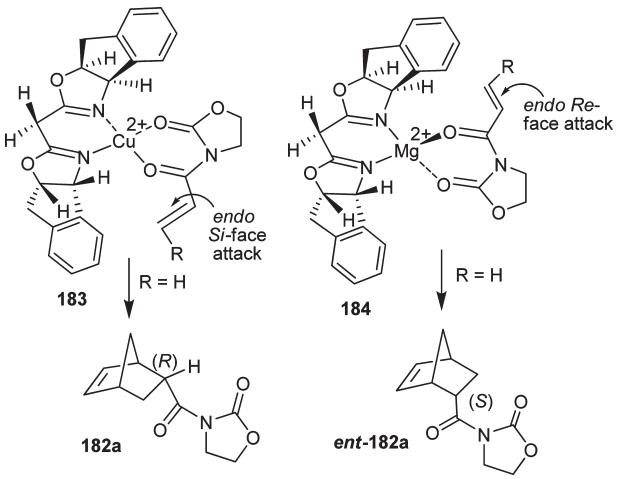

FIGURE 38. Stereochemical models for Cu(II)– and Mg(II)–bis-oxazoline-catalyzed Diels–Alder reactions.

Mg(II)-catalyzed reactions. Since 1996, bis(oxazoline) ligand **180** and its derivatives have been extensively used for a variety of other catalytic asymmetric syntheses.[101]

We have also developed cationic Pt(II)– and Pd(II)–BINAP complexes (**186**) for asymmetric Diels–Alder reactions with bidentate acyloxazolidinones and cyclopentadiene.[107] As shown in Figure 39, cationic complexes prepared by treatment of **187** with triflic acid and water provided a dramatic rate acceleration, and resulted in cycloadduct **182** (R = H) in 98% ee and 80% yield within 1 h. Pd(II)– and Pt(II)–BINAP-catalyzed reactions were rationalized by a postulated transition-state assembly as shown in **188**. The *endo-Re*-face attack is favored over the *Si*-face attack because of developing nonbonding interactions in the transition-state.[107]

We have investigated asymmetric hetero-Diels–Alder reactions using bis(oxazoline)–metal complexes with Danishefsky's diene and bidentate aldehydes such as glyoxylate ester, 1,3-dithiane-2-carboxaldehyde, and benzyloxyacetaldehyde. The reaction proceeded in a stepwise manner via a Mukaiyama aldol reaction followed by ring closing with trifluoroacetic acid (TFA) to provide dihydropyranone **190**. We have isolated and characterized both the Mukaiyama aldol product and dihydropyranone **190** prior to complete cyclization to **190** with TFA. Reactions of benzyloxyacetaldehyde provided dihydropyranone **191** in 76% yield and 85% ee (Figure 40). This was converted to the C_3–C_{14} segment **192** of laulimalide.[108]

Our investigation on α-keto esters with Danishefsky's diene provided dihydropyranone derivatives **190** in good to excellent yield and high enantioselectivity (up to 99% ee).[17] This methodology constructed a quaternary carbon center in the synthesis of marine natural product (–)-malyngolide.[17]

Asymmetric Multicomponent Reaction

We developed very efficient multicomponent reactions that provided multiple carbon–carbon bond formation leading to highly functionalized heterocycles in one-pot operation.[109] As shown in Figure 41, reactions of enol ethers **193** with bidentate aldehydes and ketones such as alkyl glyoxylate or pyruvates in the presence of $TiCl_4$ presumably provided oxocarbenium ion intermediate **194** from **193a**. This was

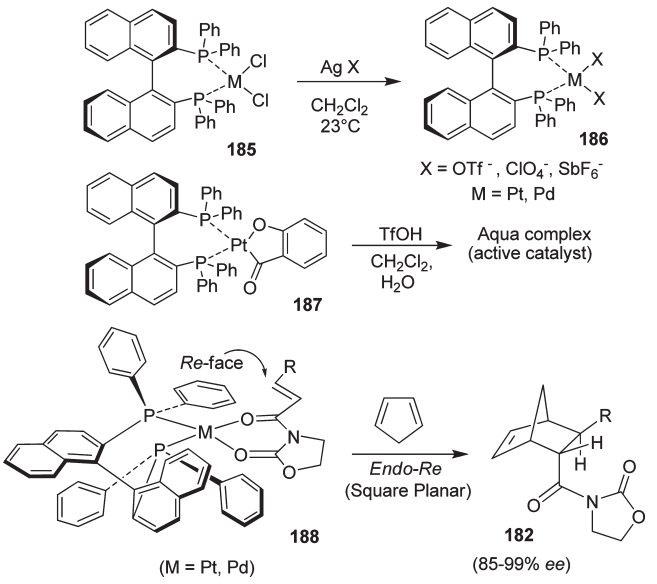

FIGURE 39. Pt(II)− and Pd(II)−BINAP complexes in Asymmetric Diels−Alder reactions.

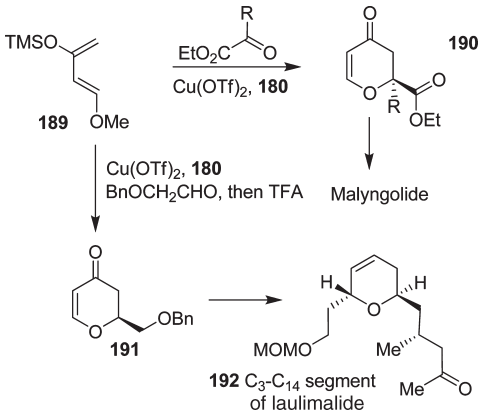

FIGURE 40. Chiral bis-oxazoline−$Cu(OTf)_2$-catalyzed hetero-Diels−Alder reactions.

trapped with a variety of nucleophiles to provide functional-

ized tetrahydrofuran and tetrahydropyran derivatives, like **195**, in good to excellent yields.[109] The overall process results in the formation of two carbon−carbon bonds and generates three chiral centers as shown in **195**. Interestingly, the reactions with pyruvates proceeded with excellent diastereoselectivity.[110] Reaction with methoxycyclohexene presumably proceeded through an oxocarbenium ion **196** and resulted in a single multicomponent product **197** with three new contiguous centers. We further investigated the potential to form carbon−carbon double bonds via the formation of an alternative oxocarbenium ion **198** upon warming the reaction to room temperature. Indeed, the reaction provided an access to a variety of α,β-unsaturated esters **199** in a single operation.[111] This reaction was utilized in a four step synthesis of (+)-eburnamonine (**9**)[16] as shown in Figure 42.

Asymmetric multicomponent reactions with optically active substituted dihydrofurans (**200**, **201**) and *N*-tosylimino ester or pyruvates also proceeded with good to excellent yields and excellent diastereoselectivity. Compound **202** was

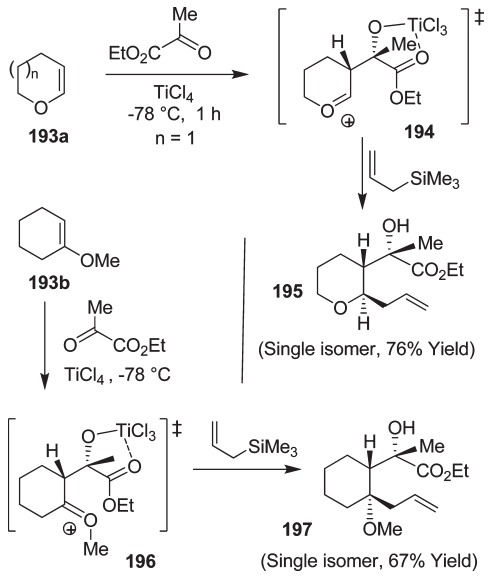

FIGURE 41. Development of new multicomponent reactions.

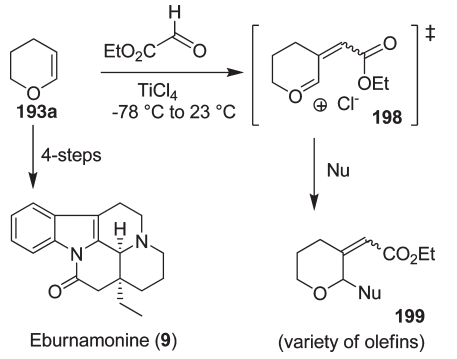

FIGURE 42. Synthesis of eburnamonine (**9**) using multicomponent reaction.

obtained as a single isomer (Figure 43).[112] Removal of the *N*-tosyl group and ester hydrolysis provided access to a variety of cyclic unnatural amino acids with multiple stereocenters.[112] We then investigated the possibility of an asymmetric multicomponent route to synthesize pyrrolidines and prolines. Multicomponent reactions with an imino ester in the presence excess of Lewis acid provided highly functionalized pyrrolidine derivative **204** in high diastereoselectivity (dr 99:1).[113] The pyrrolidine product presumably formed through the oxonium ion **203** due to the presence of excess Lewis acid. The S_N2 nucleophilic attack of the sulfonamide nucleophile (NTs^-) to the carbon center of a Lewis acid-activated oxonium ion leads to pyrrolidine **204**. A variety of substituted pyrrolidines have been prepared in a one-pot operation.[113] An asymmetric multicomponent reaction of optically active dihydrofuran **201** with ethyl pyruvate provided our presumed oxocarbenium ion, which was reacted with purine and pyrimidine bases to provide modified nucleosides in high diastereoselectivity and good yields.[114] Reaction with glyoxylate afforded a 1:1 mixture of diastereomers. The corresponding reaction with pyruvate provided **205** with excellent diastereoselectivity (dr 99:1).[114] Various asymmetric multicomponent reactions thus provided functionalized tetrahydrofurans with multiple stereogenic centers in a highly diastereoselective manner.

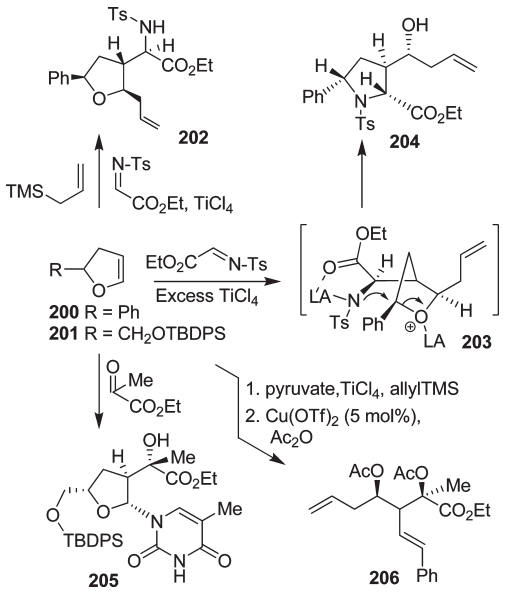

FIGURE 43. Asymmetric multicomponent reactions.

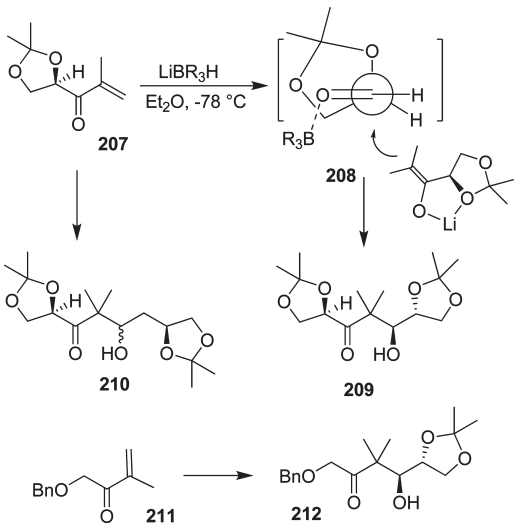

FIGURE 44. Highly diastereoselective asymmetric reductive aldol reaction.

To further broaden the scope and utility of the multicomponent reaction, we have investigated Lewis acid catalyzed cleavage of the tetrahydrofuran ring through an acyloxy carbenium ion intermediate to provide acyclic derivatives **206** with three contiguous stereogenic centers. Ring-closing olefin metathesis of such an intermediate provided access to cyclopentene derivatives or other designed molecules.[115]

Asymmetric Reductive Aldol Reaction

Recently, we have developed a highly diastereoselective asymmetric reductive aldol reaction.[116] As shown in Figure 44, aldol reaction of the enolate generated by addition of L-Selectride to enone **207** and isopropylidene-D-glyceraldehyde in ether at −78 °C provided single diastereomer, **209**, in 70% yield. Reaction with chiral isopropylidenebutyraldehyde, however, provided a 1:1 mixture of diastereomers. The corresponding reaction with isovaleraldehyde provided a 1:1 mixture of diastereomers, suggesting that the α-chirality of the isopropylidene-D-glyceraldehyde is responsible for the diastereoselectivity as proposed in the stereochemical model **208**.[116] Indeed, reaction with an achiral enone **211** and isopropylidene-D-glyceraldehyde provided single isomer **212**. This asymmetric reductive aldol reaction was utilized in the synthesis of pelorusides A and B.[31,32]

Nature-Inspired Molecular Design for Today's Medicine

Our natural product syntheses have inspired our development of new synthetic methodologies. Such research endeavors, in general, have undeniably had a profound impact in medicine and society.[117] The seemingly endless beauty, structural features, and associated bioactivity of natural products brought a unique perspective to our design and studies of diverse molecular probes relevant to today's medicine. As I have already pointed out, the majority of our synthesized targets in Figures 1 and 2 do not contain any peptide-like features; however, these molecules bind to their respective biosynthetic enzymes or target proteins or receptors with high affinity. In essence, they often compete against the natural peptide substrates to exhibit an inhibitory effect. Therefore, certain structural features, scaffolds, and templates must be involved in mimicking peptide bonds and side-chain conformations. One of our molecular design objectives is to harness nature's insight and design novel nonpeptidic molecular probes with natural-product-derived templates. A particularly intriguing possibility has been the use of conformationally constrained cyclic ethers or sulfones as surrogates of peptide carbonyl bonds. The premise here is that suitably positioned ether oxygens or sulfone oxygens can form hydrogen bonds in the enzyme's active site similar to a peptide carbonyl oxygen, while the cyclic structure would fill in the hydrophobic pocket effectively. Such a molecular design strategy may lead to molecules with enhanced pharmacological properties and metabolic stability compared to peptide-like compounds. These structural templates are inherent to numerous bioactive natural products such as monensin A (**216**),[118] ginkgolides,[119] and azadirachtin.[120] Needless to say, nature has been optimizing such templates for millions of years in various biological micro-environments. Of course, we are cognizant that such a seemingly academic approach to medicinal chemistry may not be attractive in industry due to complexity of design, low probability of success, and challenges associated with the synthesis of such molecules. However, my students and postdoctoral colleagues are often quite motivated in this line of research, dealing with stereochemical complexity, challenges in synthesis, and potential applications in human medicine. Our broad synthetic expertise has effectively served as a good complement to our molecular design capabilities.

Our initial focus has been in the area of structure-based design of HIV-1 protease inhibitors for the treatment of HIV infection/AIDS.[121] Our molecular design strategy for HIV protease inhibitors has been based upon X-ray structures of inhibitor-bound HIV-1 protease complexes. Of particular note, our critical analysis of the saquinavir **213**-bound protease X-ray structure led us to design a potent cyclic sulfone-derived lead **214** (Figure 45).[122,123]

Subsequently, we designed stereochemically defined spiro ethers and spiro ketal-containing potent inhibitors. As

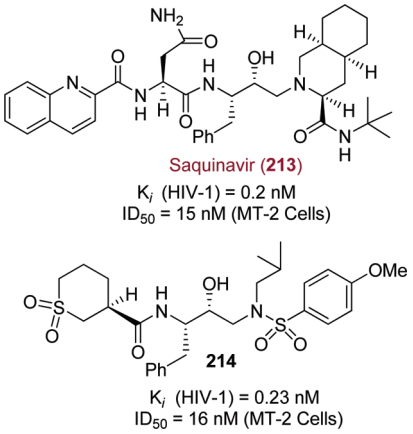

FIGURE 45. Structure of saquinavir (**213**) and cyclic sulfone **214** lead structure.

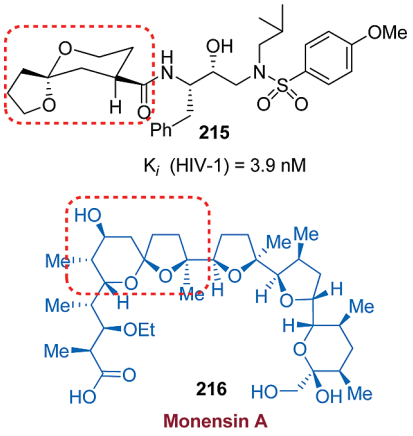

FIGURE 46. Structures of spiro ketal-derived inhibitor **215** and monensin A.

shown in Figure 46, inhibitor **215** incorporated structural features of monensin A (**216**).[3,124]

We have also designed a bicyclic fused tetrahydrofuran (bis-THF) as a high-affinity ligand for the HIV-1 protease substrate binding site. Inhibitor **217** (UIC-94017 or TMC114) shown in Figure 47 has been exceedingly potent in enzyme inhibitory and antiviral assays.[125,126] This class of inhibitors was designed to maximize interactions in the protease active site especially to form a network of hydrogen bonds with the protease backbone from the S2- to S2′-subsites. This basic "backbone binding" design concept[127] evolved from our observation of reported X-ray structures that the active-site protease backbone conformation is minimally distorted across a wide variety of mutant proteases as compared to that of the wild-type HIV-1 protease. Therefore, we hypothesized that the inhibitors that form many hydrogen bonds with the protein backbone would retain their potency against mutant strains. Indeed, inhibitor **217** exhibited remarkable potency against multidrug-resistant HIV-1 variants.[128,129] Ultimately, clinical development of **217** culminated in darunavir, which was approved by the FDA in 2006, as the first treatment for patients harboring multidrug-resistant HIV strains.[130,131] Since 2008, darunavir has been approved for all patients with HIV-infection and AIDS including pediatric patients.[132] The bis-THF ligand design was inspired

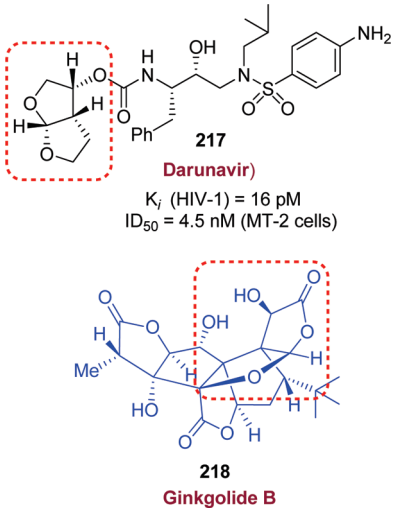

FIGURE 47. Structures of darunavir and ginkgolide B.

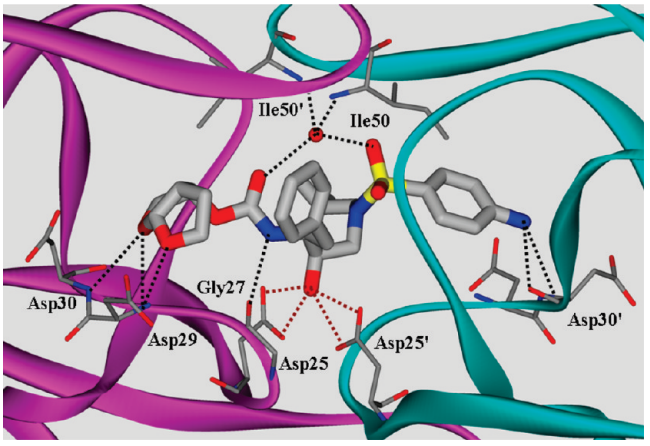

FIGURE 48. Darunavir forms an important hydrogen bonding network with the protein backbone, shown with black dotted lines.

by the structure and biology of ginkgolide natural products (Figure 47). The X-ray structure of **217**-bound HIV-1 protease was determined in collaboration with Dr. Irene Weber at Georgia State University.[133] The structure revealed (Figure 48) extensive hydrogen bonding of bis-THF ligand with the backbone atoms of the HIV-1 protease. In addition, the inhibitor makes robust interactions throughout the S2−S2′ subsites of the protease. These extensive "backbone binding" interactions may be responsible for darunavir's potency against multidrug-resistant HIV-variants.[129]

Our structure-based design strategy led to a number of other exceedingly potent inhibitors (**219**−**221**)[134−136] with diverse stereochemically defined ligands shown in Figure 49. Our work has demonstrated that the design concept targeting the protein backbone may serve as an important guide to combat drug resistance.

β-Secretase (Memapsin 2) Inhibitors for Alzheimer's Disease

Another area of focus has been our design of *β*-secretase (memapsin 2) inhibitors for the possible treatment of Alzheimer's disease (AD). Since late 1998, my laboratories have been involved in the design and synthesis of novel *β*-secretase inhibitors. *β*-Secretase is one of the two aspartyl proteases

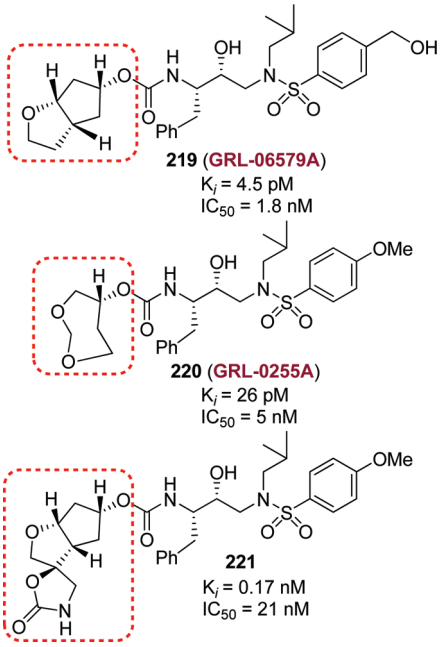

FIGURE 49. Structures of inhibitors **219**−**221**.

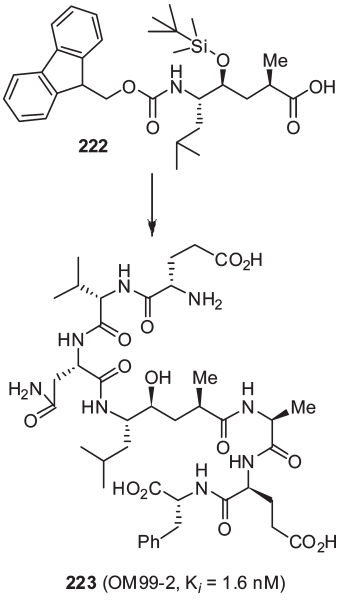

FIGURE 50. Structure of β-secretase inhibitor **223**.

that cleave the β-amyloid precursor protein (APP) to form a 40−42 amino acid amyloid-β-peptide (Aβ) in the human brain, a key event in the pathogenesis of AD.[137] In collaboration with Dr. Jordan Tang at the Oklahoma Medical Research Foundation, we have designed one of the first potent inhibitors of β-secretase based upon specificity preferences.[138] Our design strategy was to first synthesize a Leu-Ala dipeptide isostere with the *N*-terminus being Fmoc protected and the hydroxyl group as a TBS-ether (**222**, Figure 50).[138] This was used in solid-state peptide synthesis. Pseudopeptide **223** (OM 99-2) was identified by us as a very potent inhibitor of β-secretase.[138] The X-ray structure of **223**-bound β-secretase was then determined at 1.9 Å resolution by Jordan Tang and Lin Hong at the Oklahoma Medical Research Foundation.[139] This structure

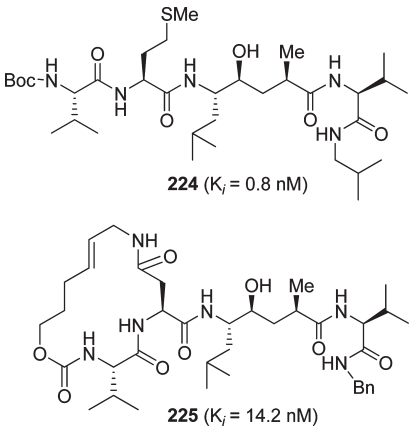

FIGURE 51. Structures of β-secretase inhibitors **224** and **225**.

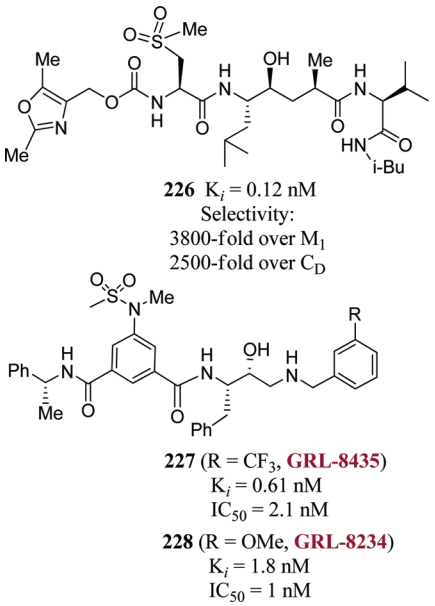

FIGURE 52. Structures of β-secretase inhibitors **226**−**228**.

provided critical molecular insights into the β-secretase active site. Based upon this structure, we subsequently reduced the molecular size and designed a number of potent and selective β-secretase inhibitors. As shown, peptidic inhibitor **224** (Figure 51) has shown a K_i of 0.8 nM. We have also designed a series of macrocyclic amide−urethanes with varying ring sizes; a representative molecule is **225**. Unfortunately, none of these inhibitors have shown any selectivity against other human aspartic acid proteases, especially against memapsin 1 (BACE2) or cathepsin D (CD).[140]

These proteases have specificity similarities with β-secretase and are involved in important physiological functions. Inhibition of these proteases would most likely lead to toxicity or consumption of inhibitor, necessitating large dose requirements. Our structure-based design efforts led to the synthesis of **226** (Figure 52), which is very potent against β-secretase and highly selective against β-secretase 2 (>3800-fold) and cathepsin D (>2500-fold).[141] An X-ray structure of the β-secretase−**226** complex revealed a number of critical molecular interactions responsible for the observed selectivity.[142] Subsequently, we designed and developed exceedingly potent small molecule inhibitors represented by **227** and **228**. Inhibitor **228** inhibited

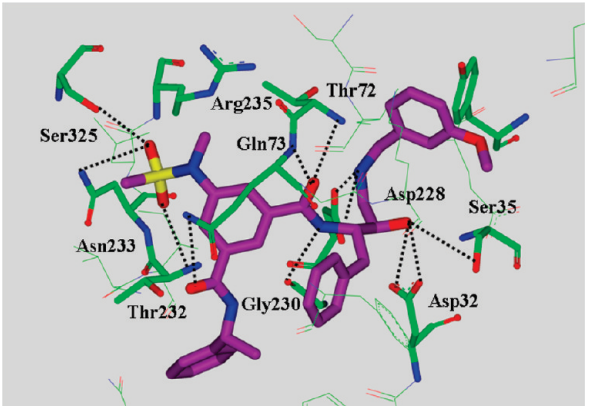

FIGURE 53. X-ray structure of **228**-bound β-secretase.

Aβ production in animal models.[143] An X-ray structure of **228**-bound β-secretase (Figure 53) has shown ligand-binding site interactions in the β-secretase active site. A number of other lead structures identified in my laboratories have been further optimized for clinical development.[144]

Conclusion

In the beginning of fall 1994, I wanted to develop a strong research program that would harness the power of organic synthesis and address the problems of today's medicine. It all started with natural products. The structural complexity, specific stereochemistry, and unique beauty of natural products have always intrigued me. But more than just the synthesis of natural products, I have been interested in exploring their biology and medicinal potential. This crossover interest led to some significant developments in my laboratories. Our synthesis of doliculide led us to define the biological mode of action of this exceedingly potent cytotoxic agent. In collaboration with Dr. Ernest Hamel at the National Cancer Institute, we determined that doliculide is an enhancer of actin assembly. This doliculide work led us to get involved with jasplakinolide synthesis and eventually persuaded us to pursue structural modification of jasplakinolide and design less complex structural variants. The synthesis of lasonolide enabled us to explore its biological mechanism of action with Dr. Yves Pommier at NCI. As it turned out, lasonolide exerts its biological action via an unprecedented mechanism that promotes chromosome condensation. This work opened up many new possibilities of therapeutic applications. The exploration of the chemistry and biology of laulimalide, and peloruside A and B has been very intriguing on numerous counts. The synthesis of laulimalide led us to explore its biological potential. Our biological studies revealed that laulimalide is a microtubule stabilizing agent like paclitaxel. However, unlike many other natural products such as the epothilones, eleutherobin, or discodermolide, laulimalide does not bind to the taxoid site. It has a distinct drug-binding site that was hitherto unknown. We have further shown in collaboration with Drs. Ernest Hamel and Evi Giannakakou that laulimalide is potent against paclitaxel and epothilone-resistant cell lines. In addition, we have shown that laulimalide is a rare microtubule stabilizing agent, which has shown synergistic effects with paclitaxel. Our pelorusides A and B syntheses also led us to explore their biological and medicinal potential. Incidentally, peloruside A and B bind to the same drug-binding site as laulimalide. This opened up an intriguing possibility of designing laulimalide and peloruside A based novel microtubule-stabilizing agents.

In conjunction with natural product syntheses, we have developed a number of new synthetic methodologies with the use of optically active *cis*-1-aminoindan-2-ol. These include asymmetric *syn*- and *anti*-aldol reactions and Diels−Alder and hetero-Diels−Alder reactions. Our ester-derived Ti-enolate-based *anti*- and *syn*-aldol processes are quite practical, and the potential of these reactions has been demonstrated through the synthesis of numerous bioactive molecules. Our catalytic asymmetric reactions with aminoindanol-derived chiral bis-oxazoline ligands resulted in the development of effective Cu- and Mg-catalyzed Diels−Alder and hetero-Diels−Alder reactions. This initial work laid the foundation for the development of many other asymmetric processes. The design and development of multicomponent reactions resulted in the generation of multiple stereocenters by carbon−carbon bond formation in a single operation. Our subsequent acyloxy carbenium ion-based ring-opening reactions provided acyclic intermediates with multiple stereocenters and further expanded the synthetic potential of these multicomponent reactions.

The chemistry and biology of natural products brought a unique perspective and motivation toward the synthesis of natural product-derived templates, scaffolds, and ligands for aspartic acid proteases involved in the pathogenesis of many human diseases. It started out as a seemingly academic endeavor where we planned to mimic peptide and peptide-like bonds with stereochemically defined cyclic ethers inspired from natural products like the ginkgolides and monensin A. This turned out to be a very gratifying investigation. This endeavor led us to develop a series of exceptionally potent HIV-1 protease inhibitors incorporating conceptually new and unprecedented cyclic ether-based nonpeptidic ligands for the protease substrate binding site. Our analysis of the X-ray structures of mutant proteases and our molecular design strategy led us to develop and investigate the "backbone binding" concept to combat drug-resistance. The design and development of darunavir as a first treatment of drug-resistant HIV is a truly humbling and gratifying experience. It is satisfying to know that darunavir may be helping many HIV/AIDS patients with few or no other possible treatment options.

Another significant development in my laboratories is our work in the design of β-secretase inhibitors for the treatment of Alzheimer's disease. We designed the first substrate-based potent inhibitor for β-secretase. Our collaborative effort with Dr. Jordan Tang also led to determination of the first X-ray structure of an inhibitor-bound β-secretase. This structure provided important drug-design templates for the structure-based design of β-secretase inhibitors. We then utilized our broad synthetic and molecular design experience to develop novel small molecule inhibitors exhibiting selectivity over other human aspartyl proteases. A number of inhibitors that evolved from my laboratories were further investigated for clinical development. Our broad synthetic experience complements our expanded design capabilities. This line of research also became a very motivating factor to graduate students and postdoctoral colleagues in my laboratories. We will continue to draw inspiration from nature

and invoke the power of organic synthesis to address new challenges.

Acknowledgment. I am very honored to receive the 2010 ACS Arthur C. Cope Scholar Award. I would like to express my deep appreciation to my many colleagues whose names appear on the cited publications. My sincere thanks and appreciation go to Drs. Ernest Hamel, Hiroaki Mitsuya, Jordan Tang, and Irene Weber for our decade-long stimulating collaboration. Also, I would like thank my faculty colleagues and friends for their support. I want to express my gratitude and thanks to my family, my wife Jody and three children, for their love and support. They are my joy and spirit. Thanks to Heather Miller for her help with the preparation of this manuscript. The financial support by the National Institutes of Health (GM53386, GM55600, and AG18933) is gratefully acknowledged.

References

(1) Ghosh, A. K. *J. Med. Chem.* **2009**, *52*, 2163–2176.
(2) (a) Danishefsky, S. L. *Nat. Prod. Rep.* **2010**, *27*, 1114–1116. (b) Lam, K. S. *Trends Microbiol.* **2007**, *15*, 279–289. (c) Gunatilaka, A. A. L. *J. Nat. Prod.* **2007**, *69*, 509–526. (d) Koehn, F. E.; Carter, G. T. *Nat. Rev. Drug Discov.* **2005**, *3*, 206–220.
(3) (a) Fenical, W.; Jensen, P. R. *Nature Chem. Biol.* **2006**, *2*, 666–673. (b) Wilson, R. M.; Danishefsky, S. J. *J. Org. Chem.* **2006**, *71*, 8329–8351. (c) Paterson, I.; Anderson, E. A. *Science* **2005**, *310*, 451–453. (d) Clardy, J.; Walsh, C. *Nature* **2004**, *432*, 829–837. and references cited therein.
(4) (a) Newman, D. J.; Cragg, G. M. *J. Nat. Prod.* **2007**, *70*, 461–477. (b) Butler, M. S. *Nat. Prod. Rep.* **2005**, *22*, 162–195.
(5) Haustedt, L. O.; Mang, C.; Siems, K.; Schiewe, H. *Curr. Opin. Drug Discov. Devel.* **2006**, *9*, 445–462.
(6) Ghosh, A. K.; Liu, W.-M.; Xu, Y.; Chen, Z. *Angew. Chem., Int. Ed.* **1996**, *35*, 74–76.
(7) Ghosh, A. K.; Liu, W.-M. *J. Org. Chem.* **1996**, *61*, 6175–6182.
(8) Ghosh, A. K.; Wang, Y. *J. Chem. Soc., Perkin Trans. 1* **1999**, 3597–3601.
(9) Ghosh, A. K.; Liu, W.-M. *J. Org. Chem.* **1997**, *62*, 7908–7909.
(10) Ghosh, A. K.; Wang, Y. *J. Org. Chem.* **1999**, *64*, 2789–2795.
(11) Ghosh, A. K.; Fidanze, S. *Org. Lett.* **2000**, *2*, 2405–2407.
(12) (a) Ghosh, A. K.; Liu, C. *Chem. Commun.* **1999**, 1743–1744. (b) Ghosh, A. K.; Shurrush, K.; Kulkarni, S. *J. Org. Chem.* **2009**, *74*, 4508–4518.
(13) Ghosh, A. K.; Bischoff, A. *Org. Lett.* **2000**, *2*, 1573–1575.
(14) Ghosh, A. K.; Bischoff, A. *Eur. J. Org. Chem.* **2004**, *10*, 2131–2141.
(15) Ghosh, A. K.; Bilcer, G. *Tetrahedron Lett.* **2000**, *41*, 1003–1006.
(16) Ghosh, A. K.; Kawahama, R. *J. Org. Chem.* **2000**, *65*, 5433–5435.
(17) Ghosh, A. K.; Shirai, M. *Tetrahedron Lett.* **2001**, *42*, 6231–6233.
(18) Ghosh, A. K.; Liu, C. *Org. Lett.* **2001**, *3*, 635–638.
(19) (a) Ghosh, A. K.; Wang, Y. *J. Am. Chem. Soc.* **2000**, *122*, 11027–11028. (b) Ghosh, A. K.; Wang, Y.; Kim, J. T. *J. Org. Chem.* **2001**, *66*, 8973–8982.
(20) Ghosh, A. K.; Bischoff, A.; Cappiello, J. *Org. Lett.* **2001**, *3*, 2677–2681.
(21) Ghosh, A. K.; Lei, H. *Tetrahedron: Asymmetry* **2003**, *14*, 629–634.
(22) (a) Ghosh, A. K.; Liu, C. *J. Am. Chem. Soc.* **2003**, *125*, 2374–2375. (b) Ghosh, A. K.; Liu, C. Harmata, M., Ed.; in Strategies and Tactics in Organic Synthesis. Academic Press: New York, 2004; Vol. 5, p 255.
(23) Ghosh, A. K.; Xu, X. *Org. Lett.* **2004**, *6*, 2055–2058.
(24) Ghosh, A. K.; Swanson, L. *J. Org. Chem.* **2003**, *68*, 9823–9826.
(25) (a) Ghosh, A. K.; Gong, G. *J. Am. Chem. Soc.* **2004**, *126*, 3704–3705. (b) Ghosh, A. K.; Gong, G. *J. Org. Chem.* **2006**, *71*, 1085–1093.
(26) Ghosh, A. K.; Xi, K. *J. Org. Chem.* **2009**, *74*, 1163–1170.
(27) Ghosh, A. K.; Xi, K. *Angew. Chem., Int. Ed.* **2009**, *48*, 5372–5375.
(28) Ghosh, A. K.; Moon, D. K. *Org. Lett.* **2007**, *9*, 2425–2427.
(29) (a) Ghosh, A. K.; Gong, G. *Org. Lett.* **2007**, *9*, 1437–1440. (b) Ghosh, A. K.; Gong, G. *Chem. Asian J.* **2008**, *3*, 1811–1823.
(30) Ghosh, A. K.; Xu, C.-X. *Org. Lett.* **2009**, *11*, 1963–1966.
(31) Ghosh, A. K.; Xu, X.; Kim, J.-H.; Xu, C.-X. *Org. Lett.* **2008**, *10*, 1001–1004.
(32) Singh, A. J.; Xu, C.-X.; Xu, X.; West, L. M.; Wilmes, A.; Chan, A.; Hamel, E.; Miller, J. J.; Northcote, P. T.; Ghosh, A. K. *J. Org. Chem.* **2010**, *75*, 2–10.
(33) Ghosh, A. K.; Kulkarni, S. *Org. Lett.* **2008**, *10*, 3907–3909.
(34) Ghosh, A. K.; Li, J. *Org. Lett.* **2009**, *11*, 4164–4167.
(35) Ghosh, A. K.; Yuan, H. *Org. Lett.* **2010**, *12*, 3120–3123.
(36) Stratmann, K.; Burgoyne, D. L.; Moore, R. E.; Patterson, G. M. L.; Smith, C. D. *J. Org. Chem.* **1994**, *59*, 7219–7226.
(37) Evans, D. A. *Asymm. Synth.* **1984**, *3*, 1.
(38) Dai, C.-F.; Cheng, F.; Xu, H.-C.; Ruan, Y.-P.; Huang, P.-Q. *J. Comb. Chem.* **2007**, *9*, 386–394. and references cited therein.
(39) O'Connell, C. E.; Salvato, K. A.; Meng, Z.; Littlefield, B. A.; Schwartz, E. C. *Bioorg. Med. Chem. Lett.* **1999**, *9*, 1541–1546. and references cited therein.
(40) Fuller, R. W.; Nagarajan, R. *Biochem. Pharmacol.* **1978**, *27*, 1981–1983.
(41) Suhadolnik, R. J. *Nucleotides as Biological Probes*; Wiley: New York, 1979; pp 19−23.
(42) For synthesis of sinefungin analogues, see: (a) Barton, D. H. R.; Gero, S. D.; Lawrence, F.; Robert-Gero, M.; Quiclet-Sire, B.; Samadi, M. *J. Med. Chem.* **1992**, *35*, 63–67. (b) Barton, D. H. R.; Gero, S. D.; Negron, G.; Quiclet-Sire, B.; Samadi, M.; Vincent, C. *Nucleosides, Nucleotides* **1995**, *14*, 1619–1630. (c) Peterli-Roth, P.; Maguire, M. P.; Leon, E.; Rapoport, H. *J. Org. Chem.* **1994**, *59*, 4186–4193.
(43) Knowles, W. S.; Sabacky, M. J.; Vineyard, B. D.; Weinkauff, D. J. *J. Am. Chem. Soc.* **1975**, *97*, 2567–2568.
(44) Vorbruggen, H.; Krolikiewicz, K.; Bennua, B. *Chem. Ber.* **1981**, *114*, 1234–1255. For recent application of this reaction, see: Johnson, C. R.; Esker, J. L.; Van Zandt, M. C. *J. Org. Chem.* **1994**, *59*, 5854–5855.
(45) Johnson, R. A.; Sharpless, K. B. In *Catalytic Asymmetric Synthesis*; Ojima, I., Ed.; VCH Publishers: New York, 1993; pp 103−158.
(46) Caron, M.; Carlier, P. R.; Sharpless, K. B. *J. Org. Chem.* **1988**, *53*, 5185–5187.
(47) (a) Dong, H.; Zhang, B.; Shi, P.-Y. *Antiviral Res.* **2008**, *86*, 1–10. (b) Dong, H.; Ren, S.; Zhang, B.; Ahou, Y.; Puig-Basagoiti, F.; Li, H.; Shi, P.-Y. *J. Virol.* **2008**, *82*, 4295–4307.
(48) (a) Lodise, T. P.; Patel, N.; Lomaestro, B. M.; Rodvold, K. A.; Drusano, G. L. *Clin. Infect. Dis.* **2009**, *49*, 507–514. (b) Rybak, M. J.; Lomaestro, B. M.; Rotscahfer, J. C.; Moellering, R. C., Jr.; Craig, W. A.; Billeter, M.; Dalovisio, J. R.; Levine, D. P. *Clin. Infect. Dis.* **2009**, *49*, 325–327. (c) Service, R. F. *Science* **1995**, *270*, 724–727.
(49) Brighty, K. E.; McGuirk, P. R. *Annu. Rep. Med. Chem.* **1991**, *26*, 123–132.
(50) Weibel, E. K.; Hadvary, P.; Hochuli, E.; Kupfer, E.; Lengsfeld, H. *J. Antibiot.* **1987**, *40*, 1081–1085.
(51) Ortar, G.; Bisogno, T.; Ligresti, A.; Morera, E.; Nalli, M.; Di Marzo, V. *J. Med. Chem.* **2008**, *51*, 6970–6979. and references cited therein.
(52) Evans, D. A.; Chapman, K. T.; Carreira, E. M. *J. Am. Chem. Soc.* **1988**, *110*, 3560–3578.
(53) Smith, C. D.; Zhang, X.; Mooberry, S. L.; Patterson, G. M. L.; Moore, R. E. *Cancer Res.* **1994**, *54*, 3779–3784.
(54) Kerksiek, M. R.; Mejillano, R. E.; Schwartz, R. E.; Georg, G. I.; Himes, R. H. *FEBS Lett.* **1995**, *377*, 59–61.
(55) Corey, E. J.; Bakshi, R. K.; Shibata, S.; Chen, C.; Singh, V. K. *J. Am. Chem. Soc.* **1987**, *109*, 7925–7926.
(56) Ishiwata, H.; Sone, H.; Kigoshi, H.; Yamada, K. *Tetrahedron* **1994**, *50*, 12853–12882.
(57) Ishiwata, H.; Nemoto, T.; Ojika, M.; Yamada, K. *J. Org. Chem.* **1994**, *59*, 4710–4711.
(58) Charette, A. B.; Juteau, H. *J. Am. Chem. Soc.* **1994**, *116*, 2651–2652.
(59) Bai, R.; Covell, D. G.; Ghosh, A. K.; Liu, C.; Hamel, E. *J. Biol. Chem.* **2002**, *277*, 32165–32171.
(60) Mayer, A. M. S. *Pharmacology* **1999**, *41*, 159–164.
(61) (a) Bubb, M. R.; Senderowicz, A. J.; Sausville, E. A.; Duncan, K. L. K.; Korn, E. D. *J. Biol. Chem.* **1994**, *269*, 14869–14871. (b) Bubb, M. R.; Spector, I.; Beyer, B. B.; Forsen, K. M. *J. Biol. Chem.* **2000**, *275*, 5163–5170.
(62) Davis, F. A.; Reddy, R. E.; Szewczyk, J. M. *J. Org. Chem.* **1995**, *60*, 7037–7039.
(63) Ghosh, A. K.; Dawson, Z. L.; Moon, D. K.; Bai, R.; Hamel, E. *Bioorg. Med. Chem. Lett.* **2010**, *20*, 5104−5107.
(64) Ghosh, A. K.; Mathivanan, P.; Cappiello, J. *Tetrahedron Lett.* **1997**, *38*, 2427–2431.
(65) Mooberry, S. L.; Tien, G.; Hernandez, A. H.; Plubrukarn, A.; Davidson, B. S. *Cancer Res.* **1999**, *59*, 653–660.
(66) Ghosh, A. K.; Wang, Y. *Tetrahedron Lett.* **2001**, *42*, 3399–3404.
(67) Pryor, D. E.; O'Brate, A.; Bilcer, G.; Diaz, J. F.; Wang, Y.; Kabaki, M.; Jung, M. K.; Andreu, J. M.; Ghosh, A. K.; Giannakakou, P.; Hamel, E. *Biochemistry* **2002**, *41*, 9109–9115.
(68) Gapud, E. J.; Bai, R.; Ghosh, A. K.; Hamel, E. *Mol. Pharmacol.* **2004**, *66*, 113–121.
(69) (a) Thepchatri, P.; Cicero, D. O.; Monteagudo, E.; Ghosh, A. K.; Cornett, B.; Weeks, E. R.; Snyder, J. P. *J. Am. Chem. Soc.* **2005**, *127*, 12838–12846. (b) Mooberry, S. L.; Hilinski, M. K.; Clark, E. A.; Wender, P. A. *Mol. Pharmaceutics* **2008**, *5*, 829–839. (c) Bennett, M. J.; Barakat, K.; Huzil, J. T.; Tuszynski, J.; Schreimer, D. C. *Chem. Biol.* **2010**, *17*, 725–734. and references cited therein.
(70) West, L. M.; Northcote, P. T.; Battershill, C. N. *J. Org. Chem.* **2000**, *65*, 445–449.
(71) Hood, K. A.; West, L. M.; Rouwe, B.; Northcote, P. T.; Berridge, M. V.; Wakefield, S. J.; Miller, J. H. *Cancer Res.* **2002**, *62*, 3356–3360.
(72) Hamel, E.; Day, B. W.; Miller, J. H.; Jung, M. K.; Northcote, P. T.; Ghosh, A. K.; Curan, D. P.; Cushman, M.; Nicolaou, K. C.; Paterson, I.; Sorenson, E. J. *Mol. Pharmacol.* **2006**, *70*, 1555–1564.
(73) Jadhav, P. K.; Bhat, K. S.; Perumal, P. T.; Brown, H. C. *J. Org. Chem.* **1986**, *51*, 432–439.

(74) Kolb, H. C.; VanNieuwenhze, M. S.; Sharpless, K. B. *Chem. Rev.* **1994**, *94*, 2483–2547.
(75) Hamel, E.; Ghosh, A. K. Manuscript in preparation.
(76) Ghosh, A. K.; Shevlin, M. In *The Development of Titanium Enolate Based Aldol Reaction*; Rainer, M., Ed.; for Modern Aldol Reactions; Wiley-VCH: New York, 2004; pp 63−121.
(77) Shimojima, Y.; Hayashi, H.; Ooka, T.; Shibukawa, M. *Agric. Biol. Chem.* **1982**, *46*, 1823–1829.
(78) (a) Shimojima, Y.; Shirai, T.; Baba, T.; Hayashi, H. *J. Med. Chem.* **1985**, *28*, 3–9. (b) Shimojima, Y.; Hayashi, H. *J. Med. Chem.* **1983**, *26*, 1370–1374.
(79) For a review on isolation of the amphidinolides, see: Kobayashi, J. In *Comprehensive Natural Products Chemistry*; Mori, K., Ed.: Elsevier: New York, 1999; Vol. 8, p 619.
(80) Blackwell, H. E.; O'Leary, D. J.; Chatterjee, A. K.; Washenfelder, R. A.; Bussmann, D. A.; Grubbs, R. H. *J. Am. Chem. Soc.* **2000**, *122*, 58–71. and references cited therein.
(81) Pommier, Y.; Zhang, Y.; Ghosh, A. K. U.S. Pat. Appl. Publ. 2010, US 20100041619 A12010218.
(82) (a) Wang, J.; Soisson, S. M.; Young, K.; Shoop, W.; Kodali, S.; Galgoci, A.; Painter, R.; Parthasarathy, G.; Tang, Y. S.; Cummings, R.; Ha, S.; Dorso, K.; Motyl, M.; Jayasuriya, H.; Ondeyka, J.; Herath, K.; Zhang, C. W.; Hernandez, L.; Allocco, J.; Basilio, A.; Tormo, J. R.; Genilloud, O.; Vicente, F.; Pelaez, F.; Colwell, L.; Lee, S. H.; Michael, B.; Felcetto, T.; Gill, C.; Silver, L. L.; Hermes, J. D.; Bartizal, K.; Barrett, J.; Schmatz, D.; Becker, J. W.; Cully, D.; Singh, S. B. *Nature* **2006**, *441*, 358–361. (b) Singh, S. B.; Jayasuriya, H.; Ondeyka, J. G.; Herath, K. B.; Zhang, C. W.; Zink, D. L.; Tsou, N. N.; Ball, R. G.; Basilio, A.; Genilloud, O.; Diez, M. T.; Vicente, F.; Pelaez, F.; Young, K.; Wang, J. *J. Am. Chem. Soc.* **2006**, *128*, 11916–11920.
(83) Herath, K. B.; Attygalle, A. B.; Singh, S. B. *J. Am. Chem. Soc.* **2007**, *129*, 15422–15423.
(84) Nicolaou, K. C.; Chen, J. S.; Edmonds, D. J.; Estrada, A. A. *Angew. Chem., Int. Ed.* **2009**, *48*, 660–719.
(85) Austin, K. A. B.; Banwell, M. G.; Willis, A. C. *Org. Lett.* **2008**, *10*, 4465–4468.
(86) Tsuda, M.; Oguchi, K.; Iwamoto, R.; Okamoto, Y.; Kobayashi, J.; Fukushi, E.; Kawabata, J.; Ozawa, T.; Masuda, A.; Kitaya, Y.; Omasa, K. *J. Org. Chem.* **2007**, *72*, 4469–4474.
(87) Brown, H. C.; Bhat, K. S. *J. Am. Chem. Soc.* **1986**, *108*, 293–294.
(88) (a) Mahrwald, R., Ed. *Modern Aldol Reactions*; Wiley-VCH: New York, 2004; Vols. 1−2. (b) Carreira, E. M.; Kvaerno, L., Ed. *Classics in Stereoselective Synthesis*; Chapter 4, Wiley-VCH: New York, 2009.
(89) Ghosh, A. K.; Onishi, M. *J. Am. Chem. Soc.* **1996**, *118*, 2527–2528.
(90) Ghosh, A. K.; Fidanze, S.; Senanayake, C. H. *Synthesis* **1998**, 937–961.
(91) Evans, D. A.; Rieger, D. L.; Bilodeau, M. T.; Urpi, F. *J. Am. Chem. Soc.* **1991**, *113*, 1047–1049.
(92) Xiang, Y.; Olivier, E.; Ouimet, N. *Tetrehedron Lett.* **1992**, *33*, 457–460.
(93) Zimmerman, H. E.; Traxler, M. D. *J. Am. Chem. Soc.* **1957**, *79*, 1920–1923.
(94) Ghosh, A. K.; Kim, J.-H. *Org. Lett.* **2003**, *5*, 1063–1066.
(95) Ghosh, A. K.; Kim, J.-H. *Org. Lett.* **2004**, *6*, 2725–2728.
(96) Hong, L.; Turner, R. T.; Koelsch, G.; Ghosh, A. K.; Tang, J. *Biochem. Soc. Trans.* **2002**, *30*, 530–534.
(97) Ghosh, A. K.; Kim, J.-H. *Tetrahedron Lett.* **2001**, *42*, 1227–1231.
(98) Ghosh, A. K.; Dawson, Z. L. *Synthesis* **2009**, 2992–3003.
(99) Ghosh, A. K.; Fidanze, S. *J. Org. Chem.* **1998**, *63*, 6146–6152.
(100) Ghosh, A. K.; Mathivanan, P.; Cappiello, J. *Tetrahedron: Asymmetry* **1998**, *9*, 1–45.
(101) Hargaden, G. C.; Guiry, P. J. *Chem. Rev.* **2009**, *109*, 2505–2550.
(102) Lowenthal, R. E.; Abiko, A.; Masamune, S. *Tetrahedron Lett.* **1990**, *42*, 6005–6008.
(103) (a) Corey, E. J.; Imai, N.; Zhang, H.-Y. *J. Am. Chem. Soc.* **1991**, *113*, 728–729. (b) Corey, E. J.; Isihara, K. *Tetrahedron Lett.* **1992**, *33*, 6807–6810.
(104) (a) Evans, D. A.; Miller, S. J.; Lectka, T. *J. Am. Chem. Soc.* **1993**, *115*, 6460–6461. (b) Evans, D. A.; Murry, J. A.; Mat, P. V.; Norcross, R. D.; Miller., S. J. *Angew. Chem., Int. Ed. Engl.* **1995**, *34*, 798–800.
(105) Evans, D. A.; Miller, S. J.; Lectaka, T. *J. Am. Chem. Soc.* **1993**, *115*, 6460–6461.
(106) Ghosh, A. K.; Cho, H.; Cappiello, J. *Tetrahedron: Asymmetry* **1998**, *9*, 3688–3691.
(107) Ghosh, A. K.; Matsuda, H. *Org. Lett.* **1999**, *1*, 2157–2160.
(108) Ghosh, A. K.; Mathivanan, P.; Cappiello, J. *Tetrahedron Lett.* **1996**, *37*, 3815–3818.
(109) Ghosh, A. K.; Kawahama, R. *Tetrahedron Lett.* **1999**, *40*, 1083–1086.
(110) Ghosh, A. K.; Kawahama, R.; Wink, D. *Tetrahedron Lett.* **2000**, *44*, 8425–8428.
(111) Ghosh, A. K.; Kawahama, R. *Tetredron Lett.* **1999**, *40*, 4751–4754.
(112) Ghosh, A. K.; Xu, C.-X.; Wink, D. *Org. Lett.* **2005**, *7*, 7–10.
(113) Ghosh, A. K.; Kulkarni, S.; Xu, C.-X.; Fanwick, P. E. *Org. Lett.* **2006**, *8*, 4509–4511.
(114) Ghosh, A. K.; Kass, J. *Chem. Commun.* **2010**, *46*, 1218–1220.
(115) Ghosh, A. K.; Kulkarni, S.; Xu, C.-X.; Shurrush, K. *Tetrahedron: Asymmetry* **2008**, *19*, 1020–1026.
(116) Ghosh, A. K.; Kass, J.; Anderson, D. D.; Xu, X.; Marian, C. *Org. Lett.* **2008**, *10*, 4811–4814.
(117) Mohr, J. T.; Krout, M. R.; Stoltz, B. M. *Nature* **2008**, *455*, 323–332.
(118) Clark, M. R.; Mohandas, N.; Shohet, S. B. *J. Clin. Invest.* **1982**, *70*, 1074–1080.
(119) Nakanishi, K. *Bioorg. Med. Chem.* **2005**, *13*, 4987–5000.
(120) Donoho, A. L. *J. Anim. Sci.* **1984**, *58*, 1528–1539.
(121) Ghosh, A. K., Ed. *Aspartic Acid Proteases As Therapeutic Targets*; Wiley-VCH: New York, 2010.
(122) (a) Hong, L.; Zhang, X. C.; Hartsuck, J. A.; Tang, J. *Protein Sci.* **2000**, *9*, 1898–1904. (b) Tie, Y.; Kovalevsky, A. Y.; Boross, P.; Wang, Y. F.; Ghosh, A. K.; Tozser, J.; Harrison, R. W.; Weber, I. T. *Proteins* **2007**, *67*, 232–242.
(123) Ghosh, A. K.; Shin, D.; Swanson, L.; Krishnan, K.; Cho, H.; Hussain, K. A.; Walters, D. E.; Holland, L.; Buthod, J. *Farmaco* **2001**, *56*, 29–32.
(124) Ghosh, A. K.; Krishnan, K.; Walters, D. E.; Cho, W.; Koo, Y.; Cho, H.; Holland, L.; Buthod, J. *Bioorg. Med. Chem. Lett.* **1998**, *8*, 687–690.
(125) Ghosh, A. K.; Kincaid, J. F.; Cho, W.; Walters, D. E.; Krishnan, K.; Hussain, K. A.; Koo, Y.; Cho, H.; Rudall, C.; Holland, L.; Buthod, J. *Bioorg. Med. Chem. Lett.* **1998**, *8*, 979–982.
(126) Ghosh, A. K.; Sridhar, P. R.; Kumaragurubaran, N.; Koh, Y.; Weber, I. T.; Mitsuya, H. *ChemMedChem* **2006**, *1*, 937–950.
(127) Ghosh, A. K.; Chapsal, B. D.; Weber, I. T.; Mitsuya, H. *Acc. Chem. Res.* **2008**, *41*, 78–86.
(128) Yoshimura, K.; Kato, R.; Kavlick, M. F.; Nguyen, A.; Maroun, V.; Maeda, K.; Hussain, K. A.; Ghosh, A. K.; Gulnik, S. V.; Erickson, J. W.; Mitsuya, H. *J. Virol.* **2002**, *76*, 1349–1358.
(129) (a) Koh, Y.; Nakata, H.; Maeda, K.; Ogata, H.; Bilcer, G.; Devasamudram, T.; Kincaid, J. F.; Boross, P.; Wang, Y. F.; Tie, Y.; Volarath, P.; Gaddis, L.; Harrison, R. W.; Weber, I. T.; Ghosh, A. K.; Mitsuya, H. *Antimicrob. Agents Chemother.* **2003**, *47*, 3123–3129. (b) Amano, M.; Koh, Y.; Das, D.; Li, J.; Leschenko, S.; Wang, Y. F.; Boross, P. I.; Weber, I. T.; Ghosh, A. K.; Mitsuya, H. *Antimicrob. Agents Chemother.* **2007**, *51*, 2143–2155.
(130) Ghosh, A. K.; Dawson, Z. L.; Mitsuya, H. *Bioorg. Med. Chem.* **2007**, *15*, 7576–7580.
(131) FDA approved darunavir on June 23, 2006 as a new HIV treatment for patients who do not respond to existing drugs. See: http://www.fda.gov/bbs/topics/NEWS/2006/NEW01395.html then search p06-85.
(132) On October 21, 2008, the FDA granted traditional approval to Prezista (darunavir), coadministered with ritonavir and with other antiretroviral agents, for the treatment of HIV-1 infection in treatment-experienced adult patients. In addition to the traditional approval, a new dosing regimen for treatment-naïve patients was approved.
(133) Tie, Y.; Boross, P. I.; Wang, Y. F.; Gaddis, L.; Hussain, A. K.; Leshchenko, S.; Ghosh, A. K.; Louis, J. M.; Harrison, R. W.; Weber, I. T. *J. Mol. Biol.* **2004**, *338*, 341–352.
(134) Ghosh, A. K.; Sridhar, P. R.; Leshchenko, S.; Hussain, A. K.; Li, J.; Kovalevsky, A.; Walters, D. E.; Wedekind, J. E.; Grum-Tokars, V.; Das, D.; Koh, Y.; Maeda, K.; Gatanaga, H.; Weber, I. T.; Mitsuya, H. *J. Med. Chem.* **2006**, *49*, 5252–5261.
(135) Ghosh, A. K.; Gemma, S.; Baldridge, A.; Wang, Y. F.; Kovalevsky, A. Y.; Koh, Y.; Weber, I. T.; Mitsuya, H. *J. Med. Chem.* **2008**, *51*, 6021–6033.
(136) Ghosh, A. K.; Chapsal, B. D.; Baldridge, A.; Ide, K.; Koh, Y.; Mitsuya, H. *Org. Lett.* **2008**, *10*, 5135–5138.
(137) Selkoe, D. J. *Nature* **1999**, *399*, 23–31.
(138) Ghosh, A. K.; Shin, D.; Downs, D.; Koelsch, G.; Lin, X.; Ermolieff, J.; Tang, J. *J. Am. Chem. Soc.* **2000**, *122*, 3522–3523.
(139) Hong, L.; Koelsch, G.; Lin, X.; Wu, S.; Terzyan, S.; Ghosh, A. K.; Zhang, X. C.; Tang, J. *Science* **2000**, *290*, 150–153.
(140) (a) Turner, R. T., III; Loy, J. A.; Nguyen, C.; Devasamudram, T.; Ghosh, A. K.; Koelsch, G.; Tang, J. *Biochemistry* **2002**, *41*, 8742–8746. (b) Diment, S.; Leech, M. S.; Stahl, P. D. *J. Biol. Chem.* **1988**, *263*, 6901–6907.
(141) Ghosh, A. K.; Kumaragurubaran, N.; Hong, L.; Lei, H.; Hussain, K. A.; Liu, C. F.; Devasamudram, T.; Weerasena, V.; Turner, R.; Koelsch, G.; Bilcer, G.; Tang, J. *J. Am. Chem. Soc.* **2006**, *128*, 5310–5311.
(142) Ghosh, A. K.; Kumaragurubaran, N.; Hong, L.; Koelsch, G.; Tang, J. *Curr. Alzheimer Res.* **2008**, *5*, 121–131.
(143) Ghosh, A. K.; Kumaragurubaran, N.; Hong, L.; Kulkarni, S.; Xu, X.; Miller, H. B.; Reddy, D. S.; Weerasena, V.; Turner, R.; Chang, W.; Koelsch, G.; Tang, J. *Bioorg. Med. Chem. Lett.* **2008**, *18*, 1031–1036.
(144) Hsu, H. H.; Jacobs, A.; Yu, J.; Li, A.; Koelsch, G.; Bilcer, G.; Tolar, M.; Grove, C.; Ghosh, A. K.; Tang, J.; Hey, J. A. In Phase l Safety and Pharmacokinetic Profile of Single Doses of CTS21166 (ASP1702) in Healthy Males. *International Conference on Alzheimer's Disease* (*ICAD*), Chicago, IL, **2008**.